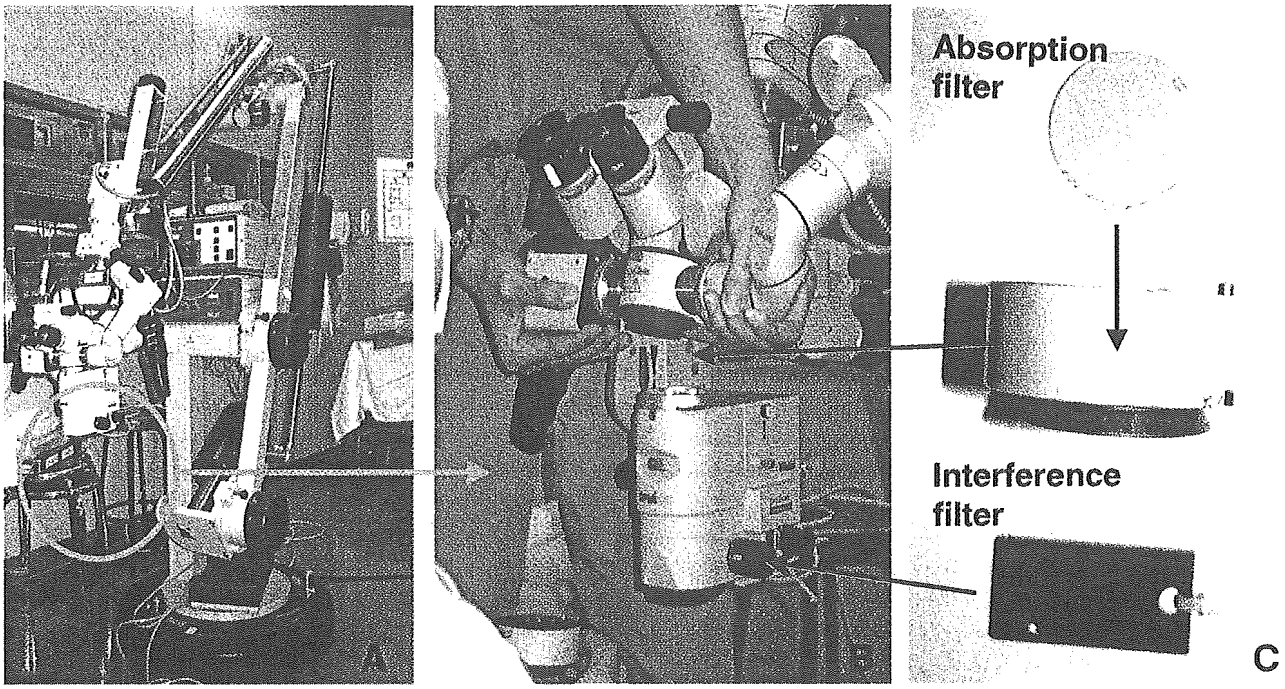

Figure 1. *The fluorescence surgical microscope used in this study. A: The whole body of the fluorescence surgical microscope manufactured by Carl Zeiss Co. Ltd.. B: Filter insertion parts. C: Absorption (>520 nm) and interference (466.5 nm) filters.*

Procedure for AO-PDT with/without low dose radiation. For Cases 1, 2, 3, 5, 9 and 10, intralesional tumor excision, similar to the conventional macroscopic curettage for benign bone or soft tissue tumors, was mainly performed, and for Cases 4, 6, 7 and 8, marginal resection of the tumor with partial intralesional excision was mainly performed. These procedures were applied, with the aim of minimizing, to the maximum extent possible, the damage to intact muscles, bones, or major nerves and vessels in close contact with the tumor, thereby obtaining good limb function after surgery. In the next step, microscopic curettage with an ultrasonic surgical knife (Olympus Co. Ltd., Tokyo, Japan) was performed additionally using a fluorescence surgical microscope, under observation of AO green fluorescence from remnant tumor fragment after local administration of 1 μg/ml of AO solution (Sigma-Aldrich Co., St. Louis, MO, USA) for 5 minutes, followed by washing out of the excess AO solution with saline and by excitation with blue light (Figure 1). The microscope was equipped with an interference filter (466.5 nm) for selection of the blue beam from a Xenon lamp, and an absorption filter (> 520 nm) for observation of the green fluorescence of AO under an ordinary surgical microscope manufactured by Carl Zeiss Co., Ltd. (Oberkochen, Germany). After repeated sessions of microscopic curettage until complete disappearance of green fluorescence from the remnant tumor mass (Figure 2), AO-PDT was applied to the tumor curettage area by illumination with blue light (5000 lx) for 10 minutes, again using the fluorescence surgical microscope. After closure of the surgical wound without washing out the AO solution, X-ray irradiation of 5 Gy in a single session was applied to the resected area immediately in 5 patients (Cases 2, 5, 7, 8, 9) in the radiotherapy room. All the 5 patients gave their consent prior to the therapy. The surgical procedures are schematically summarized in Figure 3.

The conditions of AO concentration, light illumination time and lux, and the radiation dose were decided based on the data obtained from our basic studies using a mouse model (9-12). Noteworthily, irradiation with 5 Gy was proven to be sufficient to totally kill osteosarcoma cells *in vitro* (11).

Ethical verification. This clinical trial was officially certified by the ethical committee of the Kyoto Prefectural University of Medicine, Japan. Each patient and also a close family member gave their consent for the AO-PDT with/without 5-Gy radiation after a full explanation of the method and purpose of the study (informed consent).

Study design. Before the AO-PDT with/without 5-Gy radiation, we investigated the sensitivity of each of the sarcomas to AO by using fresh biopsy specimens, which were exposed *ex vivo* to 1 μg/ml of AO solution. The therapy was administered only to those patients whose sarcoma specimens were sensitive to AO.

We principally applied this treatment to patients selected using the following criteria: patients expected to have serious deficit of limb function after wide tumor resection and limb reconstruction, or needing amputation; patients with a large tumor that could not be removed even by wide resection; patients with a high risk of death following wide tumor resection.

Evaluation of the clinical outcome. Local recurrence of tumors was evaluated by various imaging methods, such as computed tomography (CT), magnetic resonance imaging (MRI) and bone or thallium scintigraphy, and the local recurrence rate was calculated. Limb function after surgery was evaluated by the ISOLS criteria

(13). Additionally, local and systemic complications induced by AO administration, AO-PDT and AO-RDT were checked for by clinical symptoms and blood examination.

Results

All the tumor specimens studied were determined to be sensitive to AO, based on their emitting green fluorescence after *ex vivo* exposure to AO solution and blue-light excitation.

Oncologically, all the patients enrolled in this study are alive at the time of writing, without any evidence of metastatic disease. Among all the patients who were followed up for more than 2 years, local recurrence of tumor was detected in only one patient with rhabdomyosarcoma arising from the plantar aspect of the foot (Case 1). The local recurrence rate was thus 10%. However, none of the 5 patients who received AO-PDT with 5-Gy radiation developed local recurrence. The limb function of all the patients recovered to the level before surgery, except in one patient with a humeral osteosarcoma (Case 8); the recovery was, therefore, evaluated to be 100% by the ISOLS criteria in which sports activity is not needed. Even the 2 patients with a malignant bone tumor of the pelvis are able to walk well without any support.

None of the patients clinically showed local or systemic complications that could be caused by AO administration, AO-PDT with 5-Gy radiation.

Case presentation. Case 1 was 11 months old and had a rhabdomyosarcoma arising from the plantar aspect of the foot. This was probably the first human case in the world to which AO-PDT was applied for treatment. MRI revealed a large tumor mass arising from the plantar aspect of the foot, invading the interphalangeal muscles (Figure 4A). However, intensive chemotherapy with multi-anticancer agents was effective, and caused a marked decrease in the size of the tumor (Figure 4B). Therefore, secondary biopsy was performed to histologically investigate the tumor cell viability in the shrunk tumor. Histopathological examination revealed the existence of living tumor cells and *ex vivo* AO exposure also showed viable tumor cells emitting green fluorescence between muscle bundles (Figure 5), indicating that the tumor cells were sensitive to AO. Since the parents of the infant stoutly rejected the suggestion of limb amputation, we conducted tumor curettage supported by AO-PDT, as described above. Low dose radiation was not applied, because irradiation induces growth inhibition of the foot bones. MRI at 12 months after surgery showed no evidence of local tumor recurrence (Figure 6A). Three months after AO-PDT, the infant started to walk without any complications and, later, she could also run well. However, MRI at 21 months unfortunately indicated a local tumor recurrence (Figure 6B). A below knee amputation had then to be conducted, followed by repeated intensive chemotherapy, and the child is now alive with no evidence of disease.

The next case (Case 2) was a 31-year-old female patient who had a synovial sarcoma arising from the wrist. Preoperative MRI revealed that the tumor mass was in close contact with the flexor tendons and ulnar nerve (Fig 7A). If wide tumor resection had been performed for this lesion, severe dysfunction of finger motion and sensation would have been unavoidable, even after reconstruction of the tendons and nerve. Therefore, we suggested tumor curettage supported by AO-PDT with 5-Gy radiation, to the patient and her family, for preserving finger and wrist joint function. After obtaining informed consent, AO-PDT with radiation was performed. Histopathological examination of the resected tumor revealed that there were many remnant tumor cells at the tumor margin (Figure 8). Because all of the flexor tendons and ulnar nerve were completely preserved, the motor function of all the fingers and wrist joint was normally maintained and no sensory disturbance of the hand was noted. Importantly, no tumor recurrence appeared even at 4 years after the surgery (Figure 7B).

The final case (Case 9) was a patient with a huge-sized chondrosarcoma arising from the iliac bone (Figure 9). Histological findings indicated grade 2 malignant chondrosarcoma. It is commonly accepted that the prognosis of pelvic chondrosarcoma is poor, even after wide resection, because tumor embolism in the vein frequently occurs, depending on the histological grade of the malignancy (14). In this case, to perform a wide tumor resection would have been difficult, even with hemipelvectomy and, had it been performed, the limb function would have been poor and the patient would not have been able to walk. Therefore, we recommended applying AO-PDT with 5-Gy radiation to this patient after a full explanation. Both the patient and the family agreed to the treatment. At 25 months after surgery, at the time of writing, the patient still remains without tumor recurrence (Figure 10), without any complications and with no evidence of disease whatsoever. She can walk fast at present and has been able to join the same office that she worked in before the surgery.

Discussion

Acridine orange, AO, is a weak basic dye used for staining and has many unique biological activities, as previously reported, such as antitumor activity (15, 16), photosensitizing activity (17, 18), and toxic activity in bacteria, malarial parasites and fungi (19-22). It has a very low molecular weight (M.W. 463). It has also been reported that AO has the ability to rapidly flow into the cytoplasm through the cell membrane and bind to DNA (23), RNA (24) and lysosomes (25); however, our basic studies have revealed that AO binds mainly to RNA and not so avidly to DNA, emitting green fluorescence after blue light excitation in viable cultured mouse osteosarcoma cells, and also that it binds densely to lysosomes, emitting orange fluorescence (26). Because mouse osteosarcoma cells transplanted into the mouse emitted green

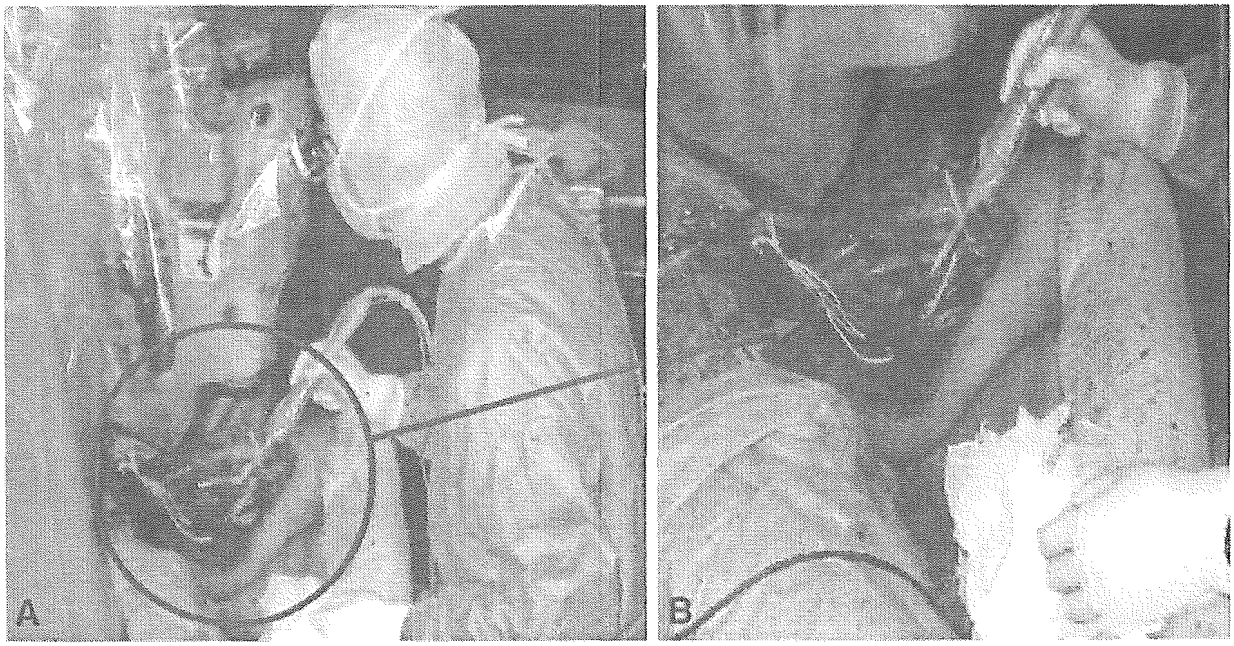

Figure 2. *Microscopic curettage after AO exposure and blue light illumination with an ultrasonic surgical knife in a patient with synovial sarcoma involving the femoral artery and vein as well as the sciatic nerve, using the fluorescence surgical microscope shown in Figure 1. The tumor was marginally resected for the most part, but the portion in contact with vessels or nerves was curetted, and additional microscopic curettage was performed under fluorovisualization with AO, followed by AO-PDT.*

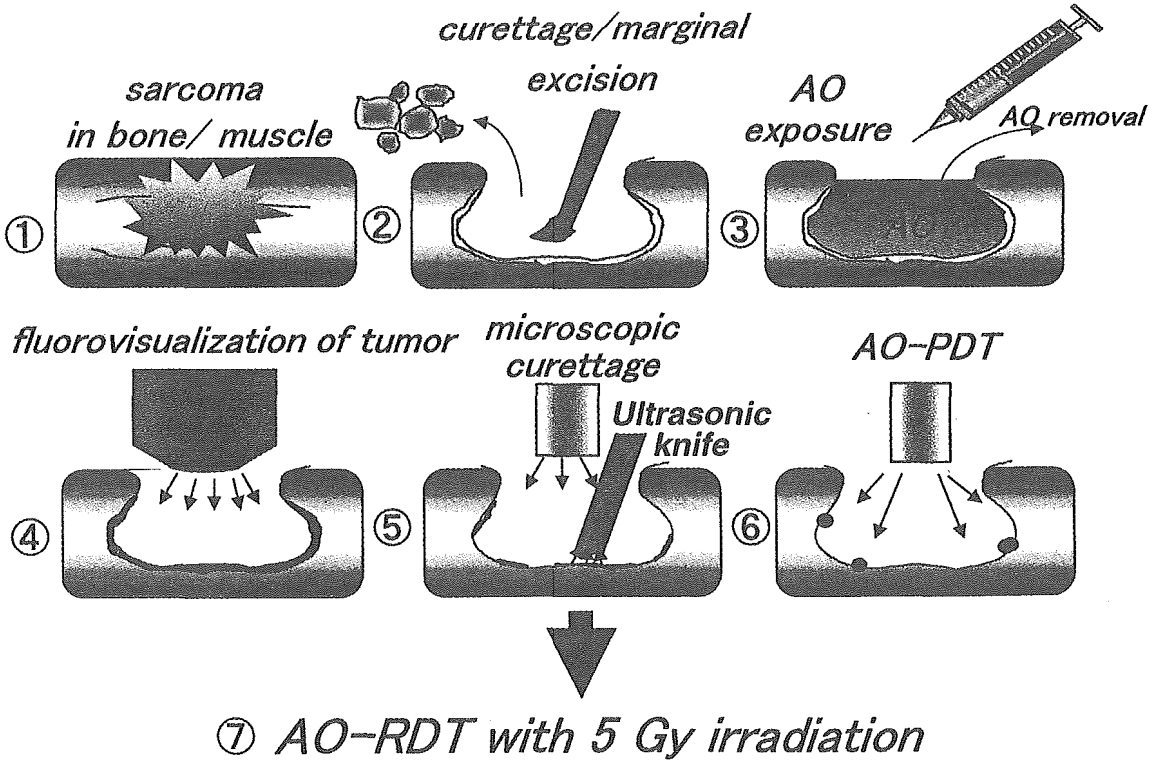

Figure 3. *Schema showing the entire procedure of AO-PDT with AO-RDT, for clinical application to human musculoskeletal sarcomas. 1. Sarcoma localized in the muscle or bone. 2. Macroscopic curettage. 3. Local administration of 1 μg/ml AO solution for exposure and removal of excessive AO solution, followed by washing out with saline. 4. Blue excitation of AO for fluorovisualization under a fluorescence surgical microscope. 5. Microscopic curettage using an ultrasonic surgical knife under visualization of green fluorescence from the remnant tumor. 6. AO-PDT by blue light illumination for 10 minutes. 7. AO-RDT by X-ray irradiation with 5 Gy.*

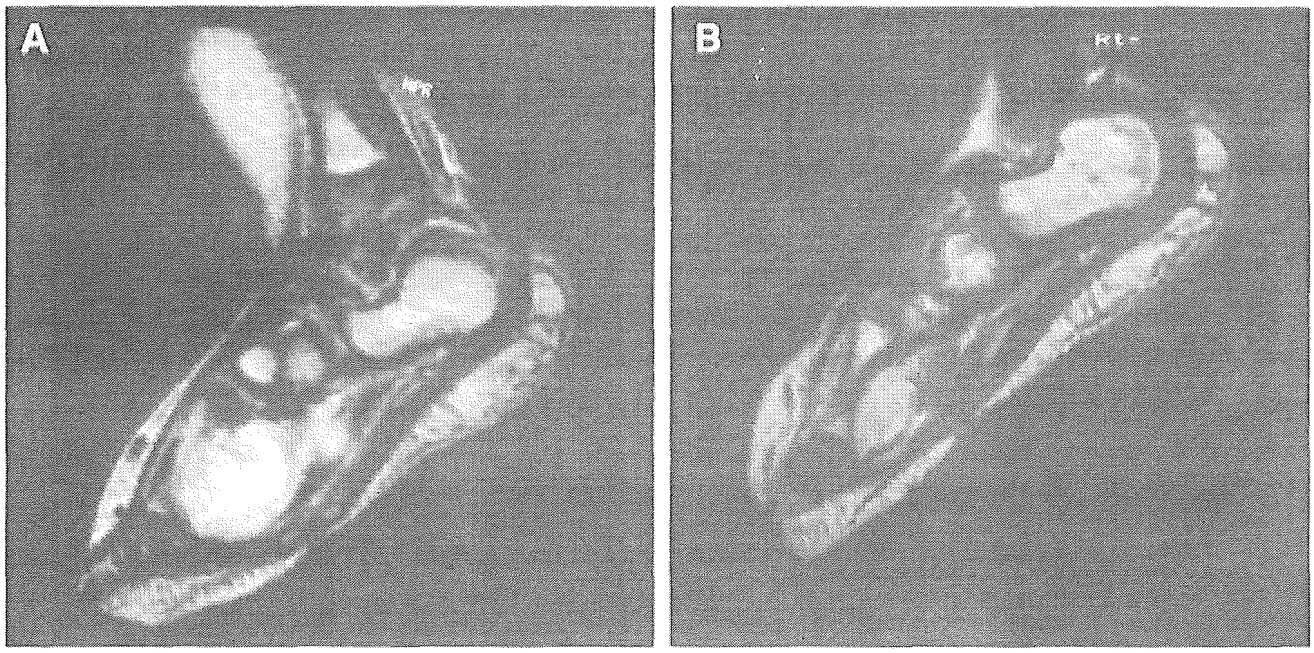

Figure 4. *MRI findings of rhabdomyosarocoma (Case 1). A: Before preoperative chemotherapy, a sagittal T2-weighted image depicted the tumor as a high signal intensity localized in the plantar region of the foot, involving muscles and metatarsal bones. B: After preoperative chemotherapy, the tumor size was remarkably decreased.*

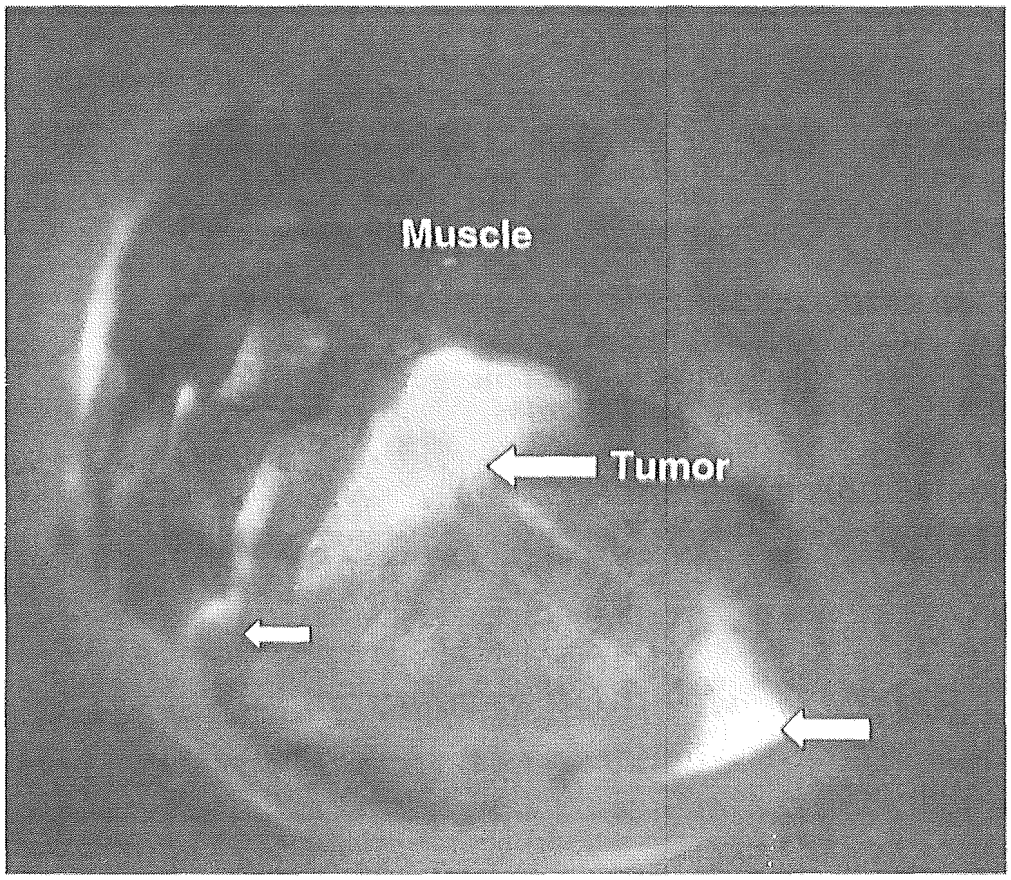

Figure 5. *Fluorescence-view from fresh remnant tumor cells invading muscle bundles obtained from the shrunk tumor tissue of Case 1, after preoperative chemotherapy, under a fluorescence surgical microscope following AO exposure and blue excitation. The remnant rhabdomyasarcoma cells emit clear green fluorescence (arrows) between the muscle bundles.*

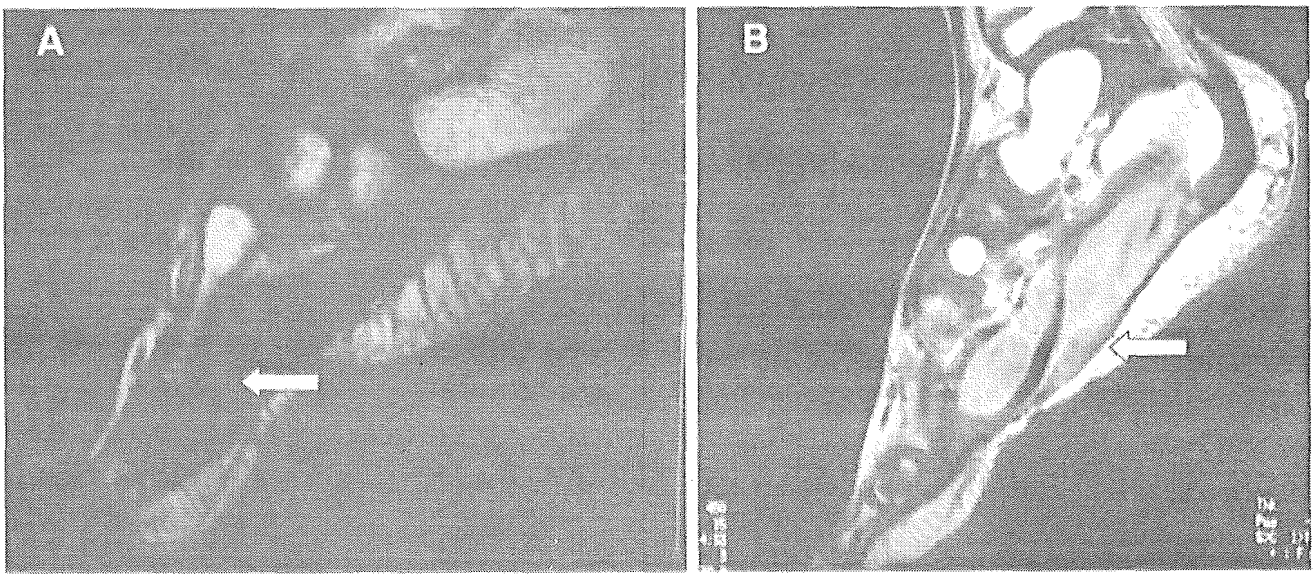

Figure 6. *MRI findings after AO-PDT in Case 1. A: Sagittal T2-weighted image at 12 months after AO-PDT showing no recurrence of tumor (arrow). B: Sagittal T1-weighted image after enhancement with gadolinium demonstrates a recurrent tumor (arrow).*

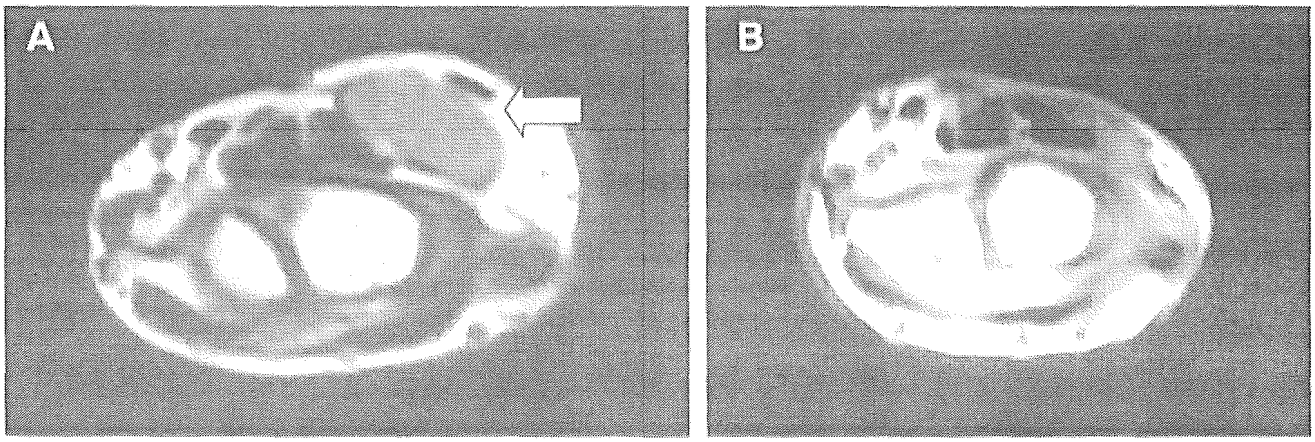

Figure 7. *MRI findings of a patient with synovial sarcoma (Case 2) arising from the wrist. A: Coronal T1-weighted image at the wrist joint before surgery shows that the tumor is in close contact with the flexor tendons in the carpal tunnel, ulnar nerve, and blood vessels. B: Coronal T1- weighted image at 48 months after AO-PDT with AO-RDT indicates that there is no tumor recurrence.*

fluorescence after intraperitoneal injection of AO followed by blue excitation, while normal muscle and adipose tissue cells did not, the tumor could be visually localized under the fluorescence surgical microscope (fluorovisualization effect) (12). We have confirmed that most human malignant bone and soft tissue tumors are sensitive to AO staining, because the surgically resected tumor specimens emit intense green fluorescence after exposure to AO solution and blue excitation. Although the mechanism underlying selective AO binding to musculoskeletal sarcomas is not clear yet, AO staining is useful for visual localization of the tumor during surgery under fluorescence microscope. We also found that AO had a strong cytocidal effect on mouse osteosarcoma cells after blue light illumination, both *in vitro* (9) and *in vivo* (10). This result suggested that AO might be useful for photodynamic therapy of musculoskeletal sarcomas. Many experimental studies previously reported that AO has properties as a photosensitizer and is useful for photodynamic therapy of cancer (27-31); however, there are, as yet, no reports of the clinical application of AO in cancer therapy. Although the reasons for this are not clearly understood, it is likely that investigators are wary of the potential toxic effects of AO, because AO has been reported to exert mutagenic activity on bacteria (19, 20). However, the carcinogenicity of AO has never yet been experimentally proven (32). An International Agency for Research on

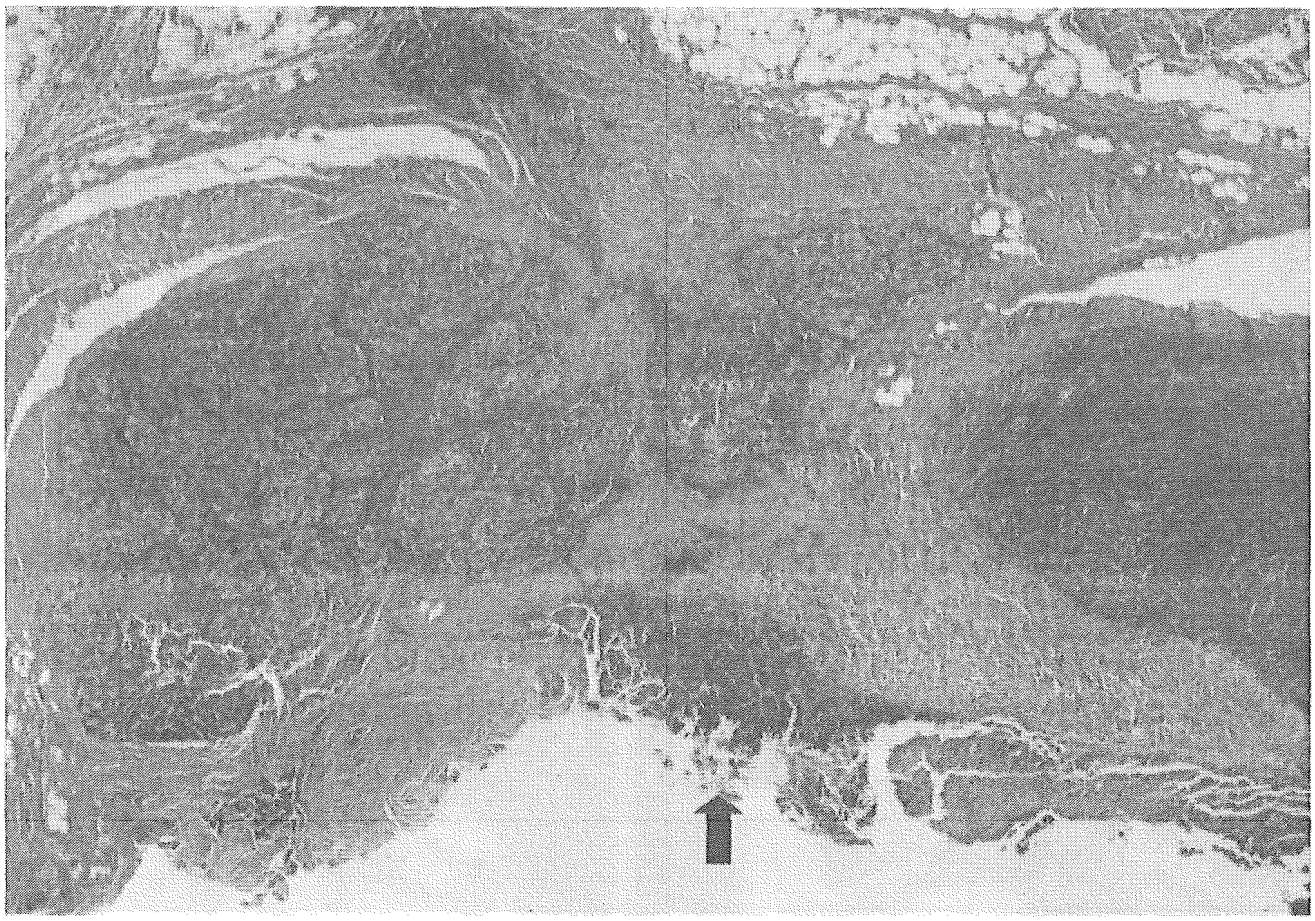

Figure 8. *Histology of the resected tumor from Case 2 (H&E stain: objective lens x 4). Because many tumor cells were seen invading the fibrous tissue surrounding the tumor mass (arrow), the surgical margin of the tumor was histologically evaluated to be intralesional.*

Cancer (IARC) report (33) in 1978 classified AO into Group 3, which means that the agent is not classifiable as to its carcinogenicity to humans. Local administration of AO to human subjects for gastric and cervical cancer screening has been reported (34), but none of the subjects have developed new cancer induced by AO. Since the concentration of AO solution used by us in this clinical study was very low, and AO was administered only locally, we believe that the risk of carcinogenesis induced by AO in our patients was probably significantly lower than that by most other known anticancer agents. Although for photodynamic therapy using porphyrin or its derivatives, which is commonly administered for various cancers (35), a laser beam which has high energy focused over a narrow area is commonly used as the excitation light source, we used a high-power Xenon lamp, because illumination of blue light over a wide area is necessary for the fluorovisualization effect of AO, as well as for a strong cytocidal effect of AO-PDT on remnant tumor cells which are widely spread throughout the surgical field by curettage. In addition, a Xenon lamp is also much cheaper than a laser. Our latest study (unpublished data) has also revealed that the cytocidal effect of AO-PDT is dependent not only on the wavelength (blue light: 466.5 nm), but also on the lux value of the light. Therefore, while blue light needs to be used for microscopic curettage, for AO-PDT, full-wave light obtained from the Xenon lamp without an interference filter is more effective than blue light alone, because of the 10- to 100-fold higher lux of the former. Since the light emitted from a Xenon lamp contains a small amount of ultra-violet or ultra-red light, the cytotoxicity on normal tissues is minimized. We have, therefore, slightly modified the methodology of AO-PDT during the last 2 years by using full-wave light.

Before clinical application of AO-PDT to human sarcomas, we performed a simulation study of curettage supported by AO-PDT, using a mouse model (10). The results showed that AO-PDT after macroscopic and microscopic curettage of a mouse osteosarcoma significantly inhibited local tumor recurrence. While the recurrence rate was 80% in the control group, it was 23% in the treated group receiving AO-PDT. Furthermore, we also found that

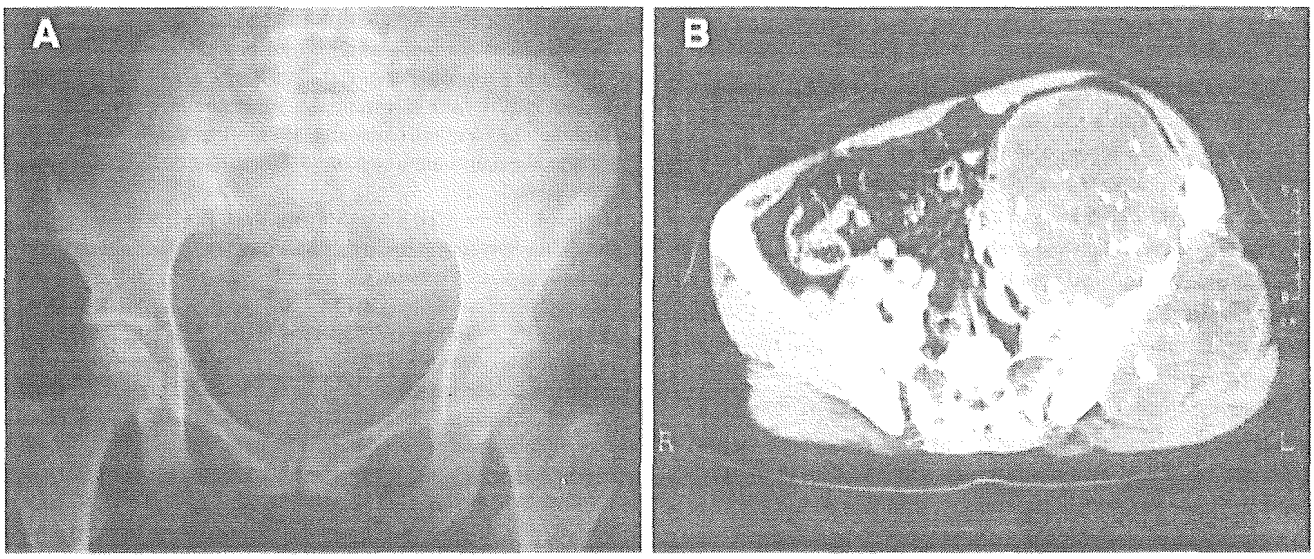

Figure 9. *Preoperative plain X-ray (A) and CT (B) of Case 9 with a chondrosarcoma (grade 2) arising from the illum. Huge tumor mass with calcification and bone destruction expands both towards the outside and internally.*

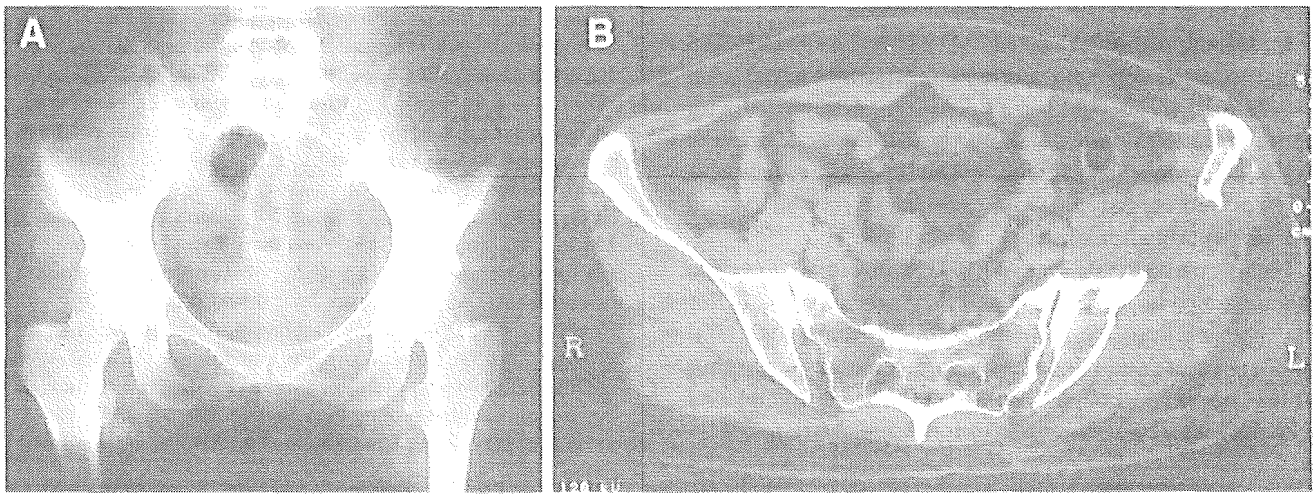

Figure 10. *Postoperative plain X-ray (A) and CT (B) of Case 9 at 24 months after AO-PDT with AO-RDT. There is no evidence of local tumor recurrence around the illium.*

low dose X-ray irradiation with 5 Gy of a mouse osteosarcoma after exposure to AO showed the same strong cytocidal effect as that of AO-PDT (11). X-ray irradiation has the advantage of reaching deeper areas of the human body than a light beam, even though it is more injurious to normal tissues. AO invades deeper tissues quickly at the rate of 1 cm per hour (unpublished data). These results of basic studies suggest that AO-PDT with low dose irradiation might be applicable for limb salvage in cases with malignant bone and soft tissue tumors. If it is effective, patients can have almost full recovery of normal limb function, with only a low risk of local recurrence.

Based on the evidence accumulated from these basic studies, after completely considering and clearing the ethical issues, we conducted a clinical study to determine the feasibility and usefulness of AO-PDT with/without low dose radiation in human musculoskeletal sarcoma patients. The results revealed an overall recurrence rate of 10% in the patients after surgery, which is almost the same as that after wide tumor resection (36-38). None of the five patients who received AO-PDT with radiation developed tumor recurrence during the follow-up period of more than 2 years. Even in the one case treated with AO-PDT alone who developed recurrence, the tumor did not recur until 21

months after the surgery, which is quite a long time when compared to that for recurrence after macroscopic curettage of high-grade malignant sarcoma. Although the follow-up duration in our study may not have been sufficient, we are convinced that the treatment protocol employed was beneficial and contend that AO-PDT with/without low dose radiation definitely has an inhibitory effect against local recurrence of musculoskeletal sarcomas, because, in general, most high-grade malignant sarcomas rapidly recur within 6 months after intralesional tumor excision (36-38). However, it still remains to be ascertained for how long this therapy might be effective.

The limb function of all patients, except for one, recovered to the baseline level after surgery, and all the patients were satisfied with this recovery. As compared with that following the presently employed limb salvage surgery with wide tumor resection followed by limb reconstruction, recovery of limb function after AO-PDT with/without low dose radiation in our study was superior. We believe that all of our patients in this study might spend the rest of their lives as normal and not handicapped people.

Local administration of AO, AO-PDT or 5-Gy radiation was not associated with any complications, such as skin hypersensitivity to light, which is often encountered with photodynamic therapy using porphyirin or its derivatives (35). Thus, with AO-PDT with/without low dose radiation, it may not be necessary to avoid exposure to the sun even in the early phase after surgery.

Finally, we conclude that AO-PDT with/without low dose radiation may be a promising new limb salvage modality for the preservation of limb function in musculoskeletal sarcoma cases, and may also be applicable to many other solid cancers, although studies on a larger number of patients with longer durations of follow-up are required.

Acknowledgements

This work was supported in part by a Grant-in-Aid (14207058) for scientific research from the Ministry of Education, Science, Sports and Culture of Japan.

References

1 Kotz R, Dominkus M, Zettl T, Ritschl P, Windhager R, Gadner H, Zielinski C and Salzer-Kuntschik M: Advances in bone tumour treatment in 30 years with respect to survival and limb salvage. A single institution experience. Int Orthop *26*: 197-202, 2002.

2 Plotz W, Rechl H, Burgkart R, Messmer C, Schelter R, Hipp E and Gradinger R: Limb salvage with tumor endoprostheses for malignant tumors of the knee. Clin Orthop *405*: 207-215, 2002.

3 Bickles J, Wittig JC, Kollender Y, Henshaw RM, Kellar-Graney KL, Meller I and Malawer MM: Distal femur resection with endoprosthetic reconstruction: a long-term follow-up study. Clin Orthop *400*: 225-235, 2002.

4 Wunder JS, Leitch K, Griffin AM, Davis AM and Bell RS: Comparison of two methods of reconstruction for primary tumors at the knee: a sequential cohort study. J Surg Oncol *77*: 89-99, 2001.

5 Rodl RW, Ozaki T, Hoffmann C, Bottner F, Linder N and Winkelmann W: Osteoarticular allograft in surgery for high-grade malignant tumors of bone. J Bone Joint Surg Br *82*: 1006-1010, 2000.

6 Lane JM, Christ GH, Khan SN and Backus SI: Rehabilitation for limb salvage patients: kinesiological parameters and psychological assessment. Cancer *92*: 1013-1019, 2001.

7 Davis AM, Sennik S, Griffin AM, Sennik S, Griffin AM, Wunder JS, O'Sullivan B, Catton CN and Bell RS: Predictors of functional outcomes following limb salvage surgery for lower-extremity soft tissue sarcoma. J Surg Oncol *73*: 206-211, 2000.

8 Refaat Y, Gunnoe J, Hornicek FJ and Mankin HJ: Comparison of quality of life after amputation or limb salvage. Clin Orthop *397*: 298-305, 2002.

9 Kusuzaki K, Minami G, Takeshita H, Murata H, Hashiguchi S, Nozaki T, Ashihara T and Hirasawa Y: Photodynamic inactivation with acridine orange on a multidrug-resistant mouse osteosarcoma cell line. Jpn J Cancer Res *91*: 439-445, 2000.

10 Kusuzaki K, Aomori, K, Suginoshita, Minami G, Takeshita H, Murata H, Hashiguchi S, Ashihara T and Hirasawa Y: Total tumor cell elimination with minimum damage to normal tissues in musculoskeletal sarcomas by photodynamic reaction with acridine orange. Oncology-Basel *59*: 174-180, 2000.

11 Hashiguchi S, Kusuzaki K, Murata H, Takeshita H, Hashiba M, Nishimura T, Ashihara T and Hirasawa Y: Acridine orange excited by low-dose radiation has a strong cytocidal effect on mouse osteosarcoma. Oncology-Basel *62*: 85-93, 2002.

12 Kusuzaki K, Suginoshita T, Minami G, Aomori K, Takeshita H, Murata H, Hashiguchi S, Ashihara T and Hirasawa Y: Fluorovisualization effect of acridine orange on mouse osteosarcoma. Anticancer Res *20*: 3019-3024 2000.

13 Enneking WF, Dunham W, Gebhardt MC, Malawar M and Prichard DJ: A system for the functional evaluation of reconstructive procedures after surgical treatment of tumors of the musculoskeletal system. Clin Orthop *286*: 241-246, 1993.

14 Pring ME, Weber KL, Unni KK and Sim FH: Chondrosarcoma of the pelvis. A review of sixty-four cases. J Bone Joint Surg Am *83*: 1630-1642, 2001.

15 Lewis RM and Goland PP: *In vivo* stainig and retardation of tumors in mice by acridine compounds. Am J Med Sci *215*: 282-289, 1948.

16 Korgaonkar K and Sukhatankara J: Anti-tumor activity of the fluorescent dye, acridine orange, on Yoshida sarcoma(ascites). Br J Cancer *17*: 471-473, 1963.

17 Zdolsek JM, Olsson GM and Brunk UT: Photooxidative damage to lysosomes of cultured macrophages by acridine orange. Photochem Photobiol *51*: 67-76, 1990.

18 Sastry KS and Gordon MP: The photodynamic inactivation of tobacco mosaic virus and its ribonucleic acid by acridine orange. Biochim Biophys Acta *129*: 32-41, 1966.

19 Zampieri A and Greenberg J: Mutagenesis by acridine orange and proflavin in *Escherichia coli* strain S. Mutat Res *2*: 552-556, 1965.

20 McCann J, Choi E, Yamasaki E and Ames BN: Detection of carcinogenesis as mutagens in the *Salmonella*/microsome test: assay of 300 chemicals. Proc Natl Acad Sci USA *72*: 5135-5139, 1975.

21 Giorgio A, Rambaldi M, Maccario P, Ambrosone L and Moles DA: Detection of microorganisms in clinical specimens using slides prestained with acridine orange (AOS). Microbiologica *12*: 97-100, 1989.
22 Rickman L, Long G, Oberst R, Cabanban A, Sangalang R, Smith J, Chulay J and Hoffman S: Rapid diagnosis of malaria by acridine orange staining of centrifuged parasites. Lancet *14*: 68-71, 1989.
23 Kapuscinski J, Darzynkiewicz Z and Melamed MR: Interactions of acridine orange with nucleic acids. Properties of complexes of acridine orange with single stranded ribonucleic acid. Biochem Pharmacol *32*: 3679-3694, 1983.
24 Amagasa J: Mechanisms of photodynamic inactivation of acridine orange-sensitized transfer RNA: participation of singlet oxygen and base damage leading to inactivation. J Radiat Res (Tokyo) *27*: 339-3351, 1986.
25 Zelenin AV: Fluorescence microscopy of lysosomes and related structures in living cells. Nature *212*: 425-426, 1966.
26 Kusuzaki K, Murata H, Takeshita H, Hashiguchi S, Nozaki T, Emoto K, Ashihara T and Hirasawa Y: Intracellular binding sites of acridine orange in living osteosarcoma cells. Anticancer Res *20*: 971-976, 2000.
27 Tomson SH, Emmett EA and Fox SH: Photodestruction of mouse epithelial tumors after oral acridine orange and argon laser. Cancer Res *34*: 3124-3127, 1974.
28 Tatsuta M, Yamamura H, Yamamoto R, Ichii M, Noguchi S, Iishi H, Mishima H, Hattori T and Okuda S: Destruction of implanted gastric tumors in rats by acridine orange photoactivation with an argon laser. Eur J Cancer Clin Oncol *20*: 543-552, 1984.
29 Prosser E, Cox D, O'Kennedy R, Carroll K and van der Putten W: Effects of coumarins, haematoporphyrins and acridine orange on the viability and growth of Landshutz ascites tumour cells, in the presence and absence of photoradiation. Cancer Lett *52*: 71-77, 1990.
30 Ishikawa S, Nemoto R, Kanoh S, Kobayashi K and Ishizaka S: Photodynamic inactivation of bladder cancer cells (MGH-U1) sensitized with acridine orange and irradiated by argon laser. Tohoku J Exp Med *144*: 265-2671, 1984.
31 Zdolsek JM: Acridine orange-mediated photodamage to cultured cells. Apmis *101*: 127-132, 1993.
32 Van Duuren, Sivak A, Katz C and Melchionne S: Tumorigenecity of acridine orange. Br J Cancer *23*: 587-590, 1969.
33 International Agency for Research on Cancer. Acridine Orange. *In*: IARC Monographs Program on the Evaluation of Carcinogenic Risks to Human. Lyon: IARC Press, Lyon *16*: 145, 1978.
34 Kato A: Gastrofiberscopic diagnosis with acridie orange fluorescence. Gastroenterol Endosc *12*: 351-362, 1970.
35 Vrouenreats MB, Visser GWM, Snow GB and van Dongen GAMS: Basic principles, applications in oncology and improved selectivity of photodynamic therapy. Anticancer Res *23*: 505-522, 2003.
36 Weiss SW and Goldblum JR: Local Recurrence in Enzinger and Weiss's Soft Tissue Tumors, 4th edition. St. Louis: Mosby, pp28-32, 2001.
37 Zagar GK, Ballo MT, Pisters PW, Pollock RE, Patel SR, Benjamin RS and Evans HL: Prognostic factors for patients with localized soft-tissue sarcoma treated with conservation surgery and radiation therapy: an analysis of 225 patients. Cancer *97*: 2530-2543, 2003.
38 Duffaud F, Digue L, Mercier C, Dales JP, Baciuchka-Palmaro M, Volot F, Thomas P and Favre R: Recurrences following primary osteosarcoma in adolescents and adults previously treated with chemotherapy. Eur J Cancer *39*: 2050-2057, 2003.

Received September 20, 2004
Accepted December 20, 2004

ELSEVIER

Journal of Orthopaedic Research 23 (2005) 979–987

Journal of Orthopaedic Research

www.elsevier.com/locate/orthres

Cytological properties of stromal cells derived from giant cell tumor of bone (GCTSC) which can induce osteoclast formation of human blood monocytes without cell to cell contact

Makoto Nishimura [a,b], Kimitaka Yuasa [a,b], Kouki Mori [a,b], Noriki Miyamoto [a,b], Morihiro Ito [a], Masato Tsurudome [a], Machiko Nishio [a], Mitsuo Kawano [a], Hiroshi Komada [a], Atsumasa Uchida [b], Yasuhiko Ito [a,*]

[a] *Department of Microbiology, Mie University School of Medicine, 2-174, Edobashi, Tsu-Shi, Mie Prefecture 514-8507, Japan*
[b] *Department of Orthopaedics, Mie University School of Medicine, 2-174, Edobashi, Tsu-Shi, Mie Prefecture 514-8507, Japan*

Abstract

When human blood monocytes were cocultured with stromal cells derived from human giant cell tumor of bone (GCTSC) and a Millipore filter (0.4 μm) was interposed between monocytes and GCTSC, multinucleated giant cell formation of monocytes was induced. The multinucleated giant cells have characters as osteoclast-like cells, indicating that a soluble osteoclast-inducing factor(s) is secreted from GCTSC expressing RANK, RANKL/ODF/OPGL and TACE mRNA. Furthermore, OCIF/OPG inhibited GCTSC-induced osteoclastogenesis, showing that the RANK–RANKL system is involved in GCTSC-induced osteoclastogenesis and that soluble form of ODF/RANKL induces osteoclasts from monocytes. GCTSC expressed the cytokine mRNAs such as M-CSF, GM-CSF, IL-3, IL-4, IL-6, and IFN-γ mRNAs. None of IL-1rα, IL-1α, IL-1β, IL-2, IL-4, IL-10, IL-18, TNF-α, G-CSF and IFN-γ could be detected in all culture media. A significant amount of IL-6 could be detected in the culture media of all GCTSC. IL-8 was found in the culture media of two GCTSC and two osteosarcoma-derived cells. M-CSF was detected in all culture media. GCTSC express CaSR, and stimulation of GCTSC with either extracellular Ca^{2+} or neomycin, agonist of CaSR, augumented the expression of RANKL. Some lines of GCTSC expressed alkaline phosphatase, osteocalcin and Cbfa1, suggesting that GCTSC are intimately related to osteoblastic lineage.

Keywords: Giant cell tumor derived stromal cells; Osteoblasts; Osteocalcin; Cbfa1; Soluble RANKL

Introduction

Giant cell tumor of bone (GCT), a relatively common neoplasm in primary bone tumors, is known to have local aggressive tendencies. Histologically, it is characterized by a large number of multinucleated giant cells and macrophage-like and stromal cell-like mononuclear cells [2,8,7,13,15,32]. The histochemical and ultrastructural features of the multinucleated giant cells and the tendency of the tumors to induce osteolysis have led several authors to characterize the multinucleated giant cells as osteoclasts and classify the tumor as osteoclastoma [8,7,10–12,27,17,20,23,32]. A significant number of macrophages were found to infiltrate to GCT, and it is generally thought that the multinucleated giant cells are formed from mononuclear phagocytic precursors by cell fusion or nuclear multiplication without cell division [3,5,6].

In our previous study [22], the stromal cells derived from giant cell tumors (GCTSC) were established from human giant cell tumors of bone. When human

* Corresponding author. Tel./fax: +81 59 231 5008.
E-mail address: ito@doc.medic.mie-u.ac.jp (Y. Ito).

0736-0266/$ - see front matter © 2005 Orthopaedic Research Society. Published by Elsevier Ltd. All rights reserved.
doi:10.1016/j.orthres.2005.01.004

peripheral blood monocytes were cocultured with GCTSC, the multinucleated giant cell formation of monocytes was induced. These multinucleated giant cells exhibited tartrate-resistant acid phosphatase (TRAP) positive, expressed calcitonin receptor and showed bone resorption activity, indicating that the multinucleated giant cells have characters as osteoclast-like cells.

The RANKL/ODF/OPGL was shown to play a critical role in osteoclastogenesis. Suda et al. [28] and Udagawa et al. [31] previously showed that the cell-to-cell interaction between osteoblasts/stromal cells and osteoclast progenitors was essential for in vitro osteoclastogenesis. In addition, Yasuda et al. [33] reported that ODF is the mediator of cell-to-cell interaction. In our previous study [22], the cell-to-cell contact between GCTSC and monocytes was mandatory for osteoclastogenesis in vitro. However, it's currently become clear that soluble mediator can drive osteoclastogenesis in the absence of stromal cells, osteoblasts, or other supporting cells [21]. In this study, we tried to investigate the involvement of the RANK–RANKL system in the GCTSC-mediated osteoclastogenesis and analyzed the cytological phenotypes of GCTSC.

Methods

Giant cell tumor-derived stromal cells (GCTSC)

Tissues were obtained at the time of surgical removal from a series of five primary giant cell tumors of bone (GCT) after informed consent. Samples of each tumor were cut into small fragments and suspended in 0.0025% trypsin diluted in phosphate-buffered saline for 60 min at 37 °C. The suspension were placed and cultured in plastic dishes with RPMI 1640 supplemented with 10% fetal calf serum, and incubated at 37 °C. Non-adherent cells and tumor debris were discarded when the media were changed every 3 or 4 days. When the cells became confluent in the dish, they were detached by treatment with 0.0025% trypsin-EDTA and placed 1:2 dilution. After several passages, the multinucleated giant cells and monocytes/macrophage-like round cells progressively disappeared from the cultures, and the proliferating stromal-like cells (GCTSC) only were present after about 4 weeks. Some properties of GCTSC were described previously [22]. These cells were cultured with Dulbecco's minimum essential medium (DMEM) fortified with 5% fetal calf serum (FCS).

Other cells

HeLa and CV-1 cells, which were grown in Eagle's MEM supplemented with 5% fetal calf serum, were used as control cells. Four cell lines derived human osteosarcomas, HOS, HSOS-1, G292 and HS-1 cells, and human osteoblast cell line (hFOB) were also used in this study. These cells were cultured with Dulbecco's minimum essential medium (DMEM) fortified with 5% fetal calf serum.

Antibody and reagents

Anti-alkaline phosphatase sheep serum, anti-osteocalcin and anti-osteopontin mAbs were purchased from Cortex Biochem. (CA, USA), Haematologic Technologies Inc. (Pinewood Plaza) and American Research Products Inc. (MA, USA), respectively. Anti-RANKL and anti-CaSR polyclonal antibodies were bought from Santa Cruz Biotechnology (CA, USA) and Alpha Diagnostic International (TX, USA), respectively. Recombinant human osteoclastogenesis inhibitory factor (OCIF)/osteoprotegerin (OPG) was bought from R&D Systems (Minneapolis, USA).

Isolation of monocytes

Peripheral blood mononuclear cells (PBMC) were isolated from healthy human volunteers' heparinized whole blood by Ficoll-Hypaque density gradient centrifugation. PBMC at the interfaces were collected and suspended in RPMI 1640 with 10% fetal calf serum. To remove contaminating platelets, PBMC were washed with balanced salt solution [150 mM NaCl, 10 mM EDTA, 10 mM Tris–HCl (pH 7.5)], layered onto FCS, and then centrifuged. Adherent monocytes were obtained from PBMC by their attachment to tissue culture dishes. The purity of the monocytes ($CD14^+$ cells) isolated by Ficoll-Hypaque and adherence was approximately 90–95%. The viability of the adherent cells after removal with a cell scraper (Sumitomo Bakelite Co., Ltd., Tokyo Japan) instead of EDTA is more than 98%, as measured by trypan blue exclusion. The monocytes were cultured in RPMI 1640 supplemented with 10% FCS instead of human serum, because in previously reported studies [29] in which human serum was used, spontaneous formation of small sized-polykaryocytes of monocytes was found. Spontaneous giant cell formation was rarely detected during 4 weeks of monocyte cultivation in RPMI 1640 medium supplemented with 10% FCS.

Cocultures

The purified monocytes were indirectly cocultured with GCTSC for 14 days. Human blood monocytes ($4–5 \times 10^5$ cells) were cultured in 24 well dishes and GCTSC ($2–3 \times 10^4$ cells) were cultured in the cell-culture insert (pore size: 0.4 μm) of the same well (Falcon Inc.).

Immunocytochemistry

Immunocytochemical staining was performed using an indirect immumofluorescent technique. The cells were fixed with 3% paraformaldehyde for 15 min at room temperature and rinsed twice with PBS. The cells were permeabilized with PBS/Tween-20 (0.05%) for 30 min and washed twice with PBS. The cells were then incubated for 60 min with primary antibody and washed three times with PBS. Next, the cells were incubated with FITC-labeled secondary antibodies for 60 min, and then were washed with PBS.

Flow-cytometric analysis

About 5×10^5 cells were fixed with 3% paraformaldehyde for 15 min at room temperature and rinsed twice with PBS. Subsequently, they were incubated with 100 μl first antibody for 60 min at room temperature, and then 100 μl FITC-conjugated secondary antibody for 60 min at room temperature. Immunofluorescent-stained cells were analyzed on a FACScan (Becton–Dickinson) using Consort 30 software (Becton–Dickinson).

Alkaline phosphatase staining

The cells were fixed with fixation solution [methylalcohol (90%), formalin solution (10%), and acetic acid (0.01%)] for 5 min, and after washing with water, the cells were stained with reaction solution (fast blue RR salt 30 mg, naphthol AS-MX phosphate sodium salt 10 mg, *N,N*-dimethylformamide 4 ml, preserved buffered solution (pH 8.6) 76 ml, water 120 ml) at 37 °C for 2 h, After washing with water, the cells were further stained with 1% safranine solution. The preserved buffered solution contains 2-amino-2-methyl-1,3-propandiol 2.1 g, 1.0 M HCl 14 ml and water 86 ml.

RNA isolation and first-strand cDNA synthesis

Total cellular RNA was extracted from 10^5–10^6 cells using guanidine isothiocyanate-cesium chloride method, as described previously. Poly(A)$^+$RNA was purified by oligo(dT)-cellulose chromatography

(Pharmacia Biotech). RNA primed with specific primers was reverse-transcribed using cloned Moloney murine leukemia virus reverse transcriptase (2.5 units), 1 mM of each deoxy-NTP, 0.2 μg specific primer, 1 unit RNase inhibitor in a final volume of 15 μl. The reaction was run at 37 °C for 60 min to complete the extension reaction. The reaction mixture was heated to 90 °C for 5 min to denature the RNA-cDNA hybrids and quick-chilled on ice.

Reverse transcription-polymerase chain reaction assays (RT-PCR)

The first-strand cDNA was submitted to PCR amplification using gene-specific PCR primers as follows: β-actin (positive control), GAPDH (positive control), CD14 (negative control), RANK (receptor activator of NF-κB), RANKL (RANK ligand)/ODF (osteoclast differentiating factor)/OPGL (osteoprotegerin ligand), CaSR (calcium-sensing receptor), M-CSF (macrophage colony-stimulating factor), IL (interleukin)-6, IL-3, IL-4, IFN (interferon)-γ, GM-CSF (granulocyte-macrophage colony-stimulating factor), OPG/OCIF (osteoprotegerin/osteoclastogenesis-inhibitory factor), TACE (tumor necrosis factor (TNF)-α converting enzyme, ADAM 17), TIMP (tissue inhibitor of metalloproteinases)-3, BMP-2 (bone morphogenetic protein-2), BMP-4, osteocalcin, osteopontin, Cbfa1 (core binding factor1), alkaline phosphatase and collagen-1. PCR was performed in 50 μl reactions containing 10 mM Tris–HCl (pH 8.3), 50 mM KCl, 1.5 mM $MgCl_2$, 0.2 mM of each dNTP, 0.5 μM of each of the sense and anti-sense PCR primers, and 2.5 units of *Taq* DNA polymerase (Perkin Elmer/Cetus, Norwalk, CT). The reaction mixture was then subjected to 30 cycles of amplification in a DNA thermal cycler. Each cycle consisted of a heat-denaturation step at 94 °C for 1 min, annealing of primers at 45–55 °C (optimized for each primer pair) for 1 min, and an extension step at 72 °C for 1 min. Following completion of 30 PCR cycles, the reactions were incubated at 72 °C for 5 min. The PCR products were separated by electrophoresis on an 1.5% agarose gel and visualized by ethidium bromide staining with ultraviolet light illumination. To confirm that the PCR products were derived from target mRNA, the products were cloned using a TA cloning kit (Invitrogen, San Diego, CA) and the nucleotide sequences were analyzed.

Fusion index

To estimate the degree of cell fusion, numbers of cells or nuclei within multinucleated giant cells (≧3 nuclei/cell) were counted. Fusion index was calculated using the formula:

$$\text{Fusion index (\%)} = \frac{\text{total number of nuclei within giant cells}}{\text{total number of nuclei counted}} \times 100$$

Results

Osteoclast formation of blood monocytes by GCTSC and blocking of GCTSC-mediated osteoclastogenesis by OCIF

Human peripheral blood monocytes were cocultured with GCTSC and a Millipore filter (size 0.4 μm) was interposed between monocytes and GCTSC. Cell aggregation of monocytes was formed within 1 day, and multinucleated giant cells began to appear at approximately 3–4 days (data not shown). The polykaryocytes increased in size until 1 week of incubation, and the number of multinucleated giant cells continued to increase for 2 weeks (Fig. 1). As shown in our previous study, these multinucleated giant cells exhibited tartrate-resistant acid phosphatase (TRAP) positive, expressed calcitonin receptor mRNA and showed bone resorption activity

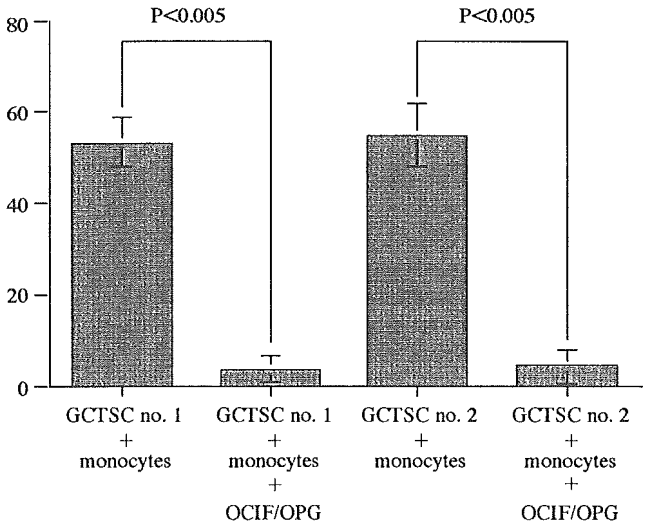

Fig. 1. Induction of osteoclast formation of blood monocytes by GCTSC and blocking of GCTSC-mediated osteoclastogenesis by OCIF. Human blood monocytes were indirectly cocultured with GCTSC no. 1 or no. 2 without or with OCIF (100 ng) for 14 days, fixed, and then stained with Giemsa solution. For quantitative analysis of multinucleated giant cell formation, fusion index was calculated.

[22]. When blood monocytes were cocultured with or without CV-1 or HeLa cells as control cells, no multinucleated giant cell was formed (data not shown). These findings indicate that GCTSC secrete soluble factor(s) inducing differentiation of monocytes to osteoclasts.

Intriguingly, when blood monocytes were indirectly cocultured with GCTSC in the presence of OCIF, GCTSC-mediated cell aggregation and osteoclastogenesis were suppressed (Fig. 1), showing that the RANK–RANKL system is involved in the GCTSC-mediated osteoclastogenesis.

Cytokine gene expression in GCTSC

Subsequently, the expression of various cytokine genes in GCTSC, blood monocytes and control cells (HeLa and CV-1 cells) was further studied using semi-quantitative RT-PCR (Fig. 2I). GCTSC expressed all the cytokine mRNAs analyzed, that is, M-CSF, GM-CSF, IL-3, IL-4, IL-6, and IFN-γ mRNAs.

Cytokine production by GCTSC

In addition, we assayed various cytokines in culture media of GCTSC and control cells (Table 1). None of IL-1rα, IL-1α, IL-1β, IL-2, IL-4, IL-10, IL-18, TNF-α, G-CSF and IFN-γ could be detected in all culture media (data not shown). A significant amount of IL-6 could be detected in the culture media of all GCTSC and control cells. A small amount of IL-8 was found in the culture media of two GCTSC and one osteosarcoma-derived cells (G292 cells). Interestingly, one of osteosarcoma-derived cells, HOS cells, produced a large quantity

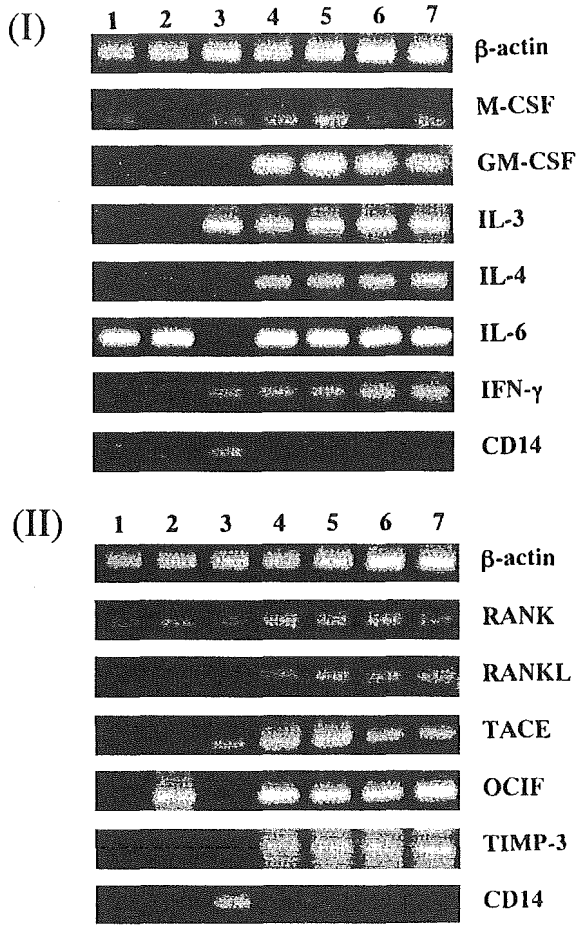

Fig. 2. I: Expression of various cytokines mRNAs in GCTSC and control cells. The expression of β-actin (positive control mRNA), M-CSF, GM-CSF, IL-3, IL-4, IL-6, IFN-γ and CD14 (negative control mRNA) in HeLa (lane 1), CV-1 cells (lane 2) and freshly isolated monocytes (lane 3), GCTSC no. 1 (lane 4), no. 2 (lane 5), no. 3 (lane 6), and no. 4 (lane 7) was analyzed by RT-PCR. II: Expression of RANK, RANKL, TACE, OCIF, and TIMP-3 mRNAs in GCTSC and control cells. The expression of β-actin (positive control mRNA), RANK, RANKL/ODF/OPGL, TACE, OCIF, TIMP-3 mRNAs and CD14 (negative control mRNA) in HeLa (lane 1), CV-1 cells (lane 2) and freshly isolated monocytes (lane 3), GCTSC no. 1 (lane 4), no. 2 (lane 5), no. 3 (lane 6), and no. 4 (lane 7) was analyzed by RT-PCR.

of IL-8 and IL-6. M-CSF was detected in all culture media.

Expression of mRNAs of RANKL-system related proteins

The RANKL/ODF/OPGL/TRANCE was shown to play a critical role in osteoclastogenesis [17,14,33]. Therefore, we tried to detect the expression of RANK, RANKL and OCIF mRNAs (Fig. 2II). Surprisingly, all GCTSC expressed RANK, RANKL and OCIF mRNAs. Since TACE has been reported to cleave RANKL, resulting in release of soluble RANKL [1,18,24], expression of TACE mRNA was investigated. Intriguingly, all GCTSC also expressed TACE mRNA (Fig. 2II). Since the tissue

Table 1
Cytokine production by giant cell tumor derived stromal cells (GCTSC)

Cell strains	Cytokine in the culture fluids (pg/ml)[a]		
	IL-6	IL-8	M-CSF
HeLa	20	<20	49
CV-1	368	<20	848
HSOS-1	<20	<20	332
G292	<20	48	227
HS-1	<20	<20	1211
HOS	6010	993	335
GCTSC-1	53	<20	186
GCTSC-2	28	<20	172
GCTSC-3	88	28	308
GCTSC-4	182	31	311

□ shows positive production.
[a] Various cells were cultured in the absences of serum for 2 days, and then the culture fluids were assayed for cytokines.

inhibitor of metalloproteinase-3 (TIMP-3) suppressed the activity of TACE [19], the expression of TIMP-3 was analyzed. Interestingly, TIMP-3 mRNA was also detected in all GCTSC (Fig. 2II).

Extracellular Ca^{2+} enhances RANKL expression in GCTSC

Extracellular Ca^{2+} is well known to regulate bone remodeling. Thus, the effect of extracellular Ca^{2+} on GCTSC was studied. At first, the expression of calcium-sensing receptor (CaSR) in GCTSC was analyzed using RT-PCR and immunofluorescent staining. As shown in Fig. 3A, the osteoblasts and osteosarcoma-derived cells express CasR mRNA. Interestingly, GCTSC also express CasR and CasR mRNA (Fig. 3A and B). Subsequently, when GCTSC were incubated with various concentrations of Ca^{2+} for 24 h, expressions of RANKL, OPG and M-CSF mRNAs were investigated. The enhanced expression of RANKL mRNA was induced by extracellular Ca^{2+} (10 mM), while the expression levels of OPG and M-CSF mRNAs were not influenced by extracellular concentration of Ca^{2+} (Fig. 4A). RANKL could be detected in GCTSC stimulated with 10 mM Ca^{2+} by an immunofluorescent method (Fig. 4C and D). In the next experiment, since the aminoglycoside antibiotic neomycin is a known agonist of CaSR, whether neomycin enhanced RANKL expression in GCTSC was tested. As shown in Fig. 4B, the neomycin evoked dose-dependent increases the expression of RANKL mRNA, but showed no/little effect on expression of OPG and M-CSF mRNAs. Furthermore, RANKL could be detected in GCTSC stimulated with the neomycin in a dose dependent manner (Fig. 4E).

Expression of mRNAs of osteoblast-marker proteins

Subsequently, we analyzed expression of mRNAs related to osteoblast markers in GCTSC (Fig. 5). The

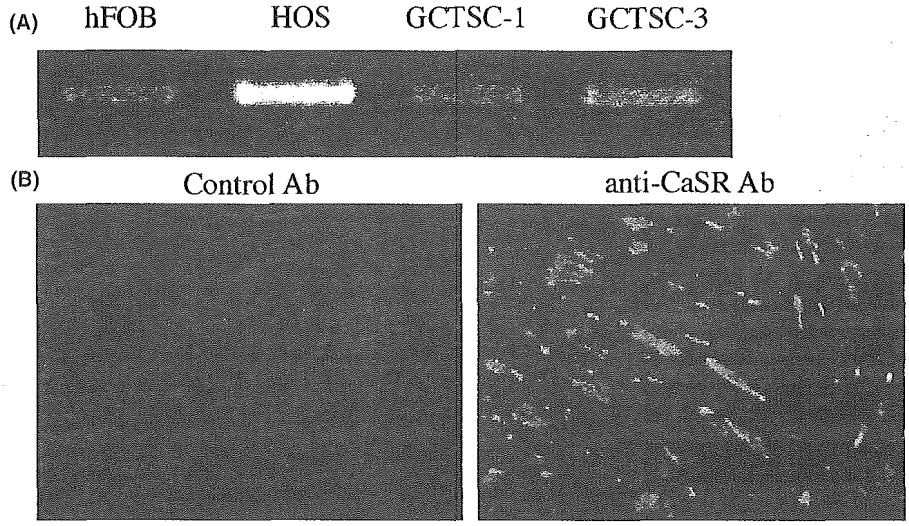

Fig. 3. Expression of CaSR mRNA, and CaSR in GCTSC. (A) The expression of CaSR mRNA in hFOB cells, HOS cells, GCTSC no. 1 and no. 3 was analyzed by RT-PCR. (B) GCTSC no. 3 were incubated with control or anti-CaSR antibody for 60 min, and then were treated with fluorescent-conjugated secondary antibody.

expression of BMP-2 was not specific for osteosarcoma-derived cells. All of GCTSC and osteosarcoma-derived cells expressed a larger quantity of BMP-4 and collagen-1 mRNAs than control cells, HeLa and CV-1 cells. Osteopontin was detected distinctly in three and faintly in one of four GCTSC. Bone specific alkaline phosphatase (ALP) mRNA was not detected in GCTSC, while all of osteosarcoma-derived cells distinctly expressed ALP mRNA. GCTSC no. 3 strongly expressed osteocalcin mRNA. Intriguingly, mRNA of osteoblast-specific transcription factor, Cbfa 1, was expressed in all of GCTSC, though the expression was lower than osteosarcoma-derived cells except G292 cells. These findings suggest that GCTSC are intimately related to osteoblastic lineage.

Alkaline phosphatase staining

In the next experiment, alkaline phosphatase staining of GCTSC was carried out. Control cells, CV-1, exhibited alkaline phosphatase (ALP) negative and four cell lines of osteosarcoma (HSOS-1, G292, HS-1 and HOS) showed ALP positive (Fig. 6 and data not shown). Interestingly, a few cells (about 5%) in GCTSC no. 3 and no. 4 exhibited ALP positive (Fig. 6 and data not shown).

Immunofluorescent analysis using anti-osteocalcin, osteopontin, and bone specific alkaline phosphatase antibodies

Immunofluorescent analysis revealed that a few cells in one of four GCTSC (no. 3) expressed osteocalcin and bone specific alkaline phosphatase (Fig. 7), indicating that some GCTSC contain the cells related to osteoblasts.

Discussion

Giant cell tumors of bone, histologically, consist of a large number of multinucleated giant cells, and macrophage-like and stromal-like mononuclear cells (GCTSC) [13,15,29,32]. The multinucleated giant cells have been characterized as osteoclasts. Prior to this study, we supposed that multinucleated giant cells in GCT arose from infiltrated monocyte/macrophage lineage cells and giant cell formation was supported by stromal cells. Consequently, we examined whether osteoclast-like cells were induced by cocultivation of blood monocytes with GCTSC which were established from giant cell tumors, showing spindle shape. When blood monocytes were cocultured with GCTSC for about 3 days, the multinucleated giant cell formation of monocytes was observed. Intriguingly, even when a filter (pore size: 0.4 μm) was interposed between monocytes and GCTSC, polykaryocytes also appeared. The multinucleated giant cells have characters as osteoclast cells. These findings indicate that soluble factor(s) secreted from GCTSC plays an important role on osteoclast-like cell formation from blood monocytes.

Suda et al. [28] and Udagawa et al. [31] previously showed that the cell-to-cell interaction between osteoblasts/stromal cells and osteoclast progenitors was essential for in vitro osteoclastogenesis, and they proposed a hypothesis that osteoblasts/stromal cells expresses a common factor, osteoclast differentiation factor(s) (ODF), in response to other osteotropic factors. They speculated that ODF appeared a

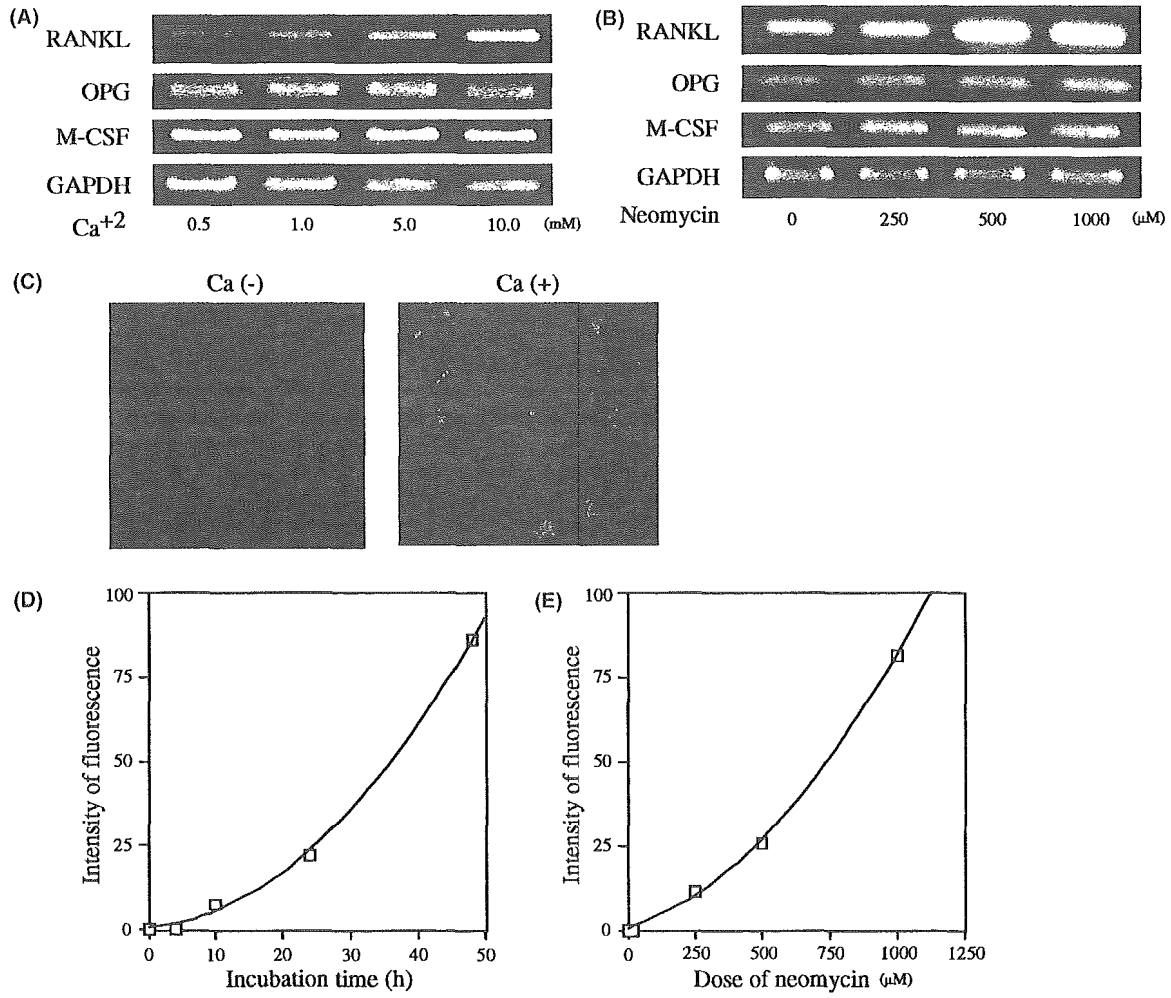

Fig. 4. Effects of extracellular Ca^{2+} and neomycin on the expression of RANKL in GCTSC. (A and B) GCTSC no. 3 were stimulated with various concentrations of extracellular Ca^{2+} (A) or neomycin (B) for 24 h. Subsequently, the expression of RANKL, OPG, M-CSF and GAPDH (control) mRNAs were analyzed by RT-PCR. (C) GCTSC no. 3 were incubated with or without 10 mM Ca^{2+} for 24 h, and then the cells were immunostained with anti-RANKL antibody. (D) GCTSC no. 3 were incubated with 10 mM extracellular Ca^{2+}, and at appropriate periods, the expression of RANKL was analyzed using a flow cytometory. (E) GCTSC no. 3 were incubated with various dose of neomycin for 24 h, and then the expression of RANKL was analyzed using a flow cytometory.

membrane-associated factor, since the cell-to-cell contact between osteoclast precursors and osteoblasts/stromal cells was prerequisite for osteoclast formation. Furthermore, M-CSF is indispensable for both the proliferative phase and differentiation phase of osteoclast development [14,17,25,33]. However, the cell-to-cell interaction was not required for the osteoclastogenesis in our present system (GCTSC-monocytes system) and in our previous system (osteosarcoma derived cells-monocytes system [21]).

GCTSC expressed a lot of cytokine mRNAs. Furthermore, mRNAs related to the RANK–RANKL system, that is, RANK, RANKL, TACE, OCIF and TIMP-3, were detected in GCTSC. The OCIF/OPG is a member of the TNF receptor family, but it does not have a transmembrane domain [26,30]. The OCIF/OPG ligand is identical to ODF (TRANCE/RANKL) and OCIF/OPG functions as a decoy receptor for ODF/RANKL, resulting in blocking RANKL activity [17,30]. Intriguingly, GCTSC-mediated osteoclastogenesis was suppressed by OCIF, indicating that the RANK–RANKL system is involved in GCTSC-mediated osteoclastogenesis. TNF-α converting enzyme (TACE; ADAM-17) is a membrane-bound disintegrin metalloproteinase [18] and TACE has been reported to be able to cleave RANKL, resulting in release of soluble RANKL [18,24]. In addition, a genetically prepared soluble form of ODF can induce differentiation of peripheral blood mononuclear cells to osteoclasts with aide of M-CSF under our experimental conditions. TACE was found to be well inhibited by tissue inhibitor of metalloproteinase-3 (TIMP-3) but not by TIMP-1, -2 and -4 [1]. Interestingly, TIMP-3 mRNA was also found in GCTSC. One of possible mechanisms by which GCTSC

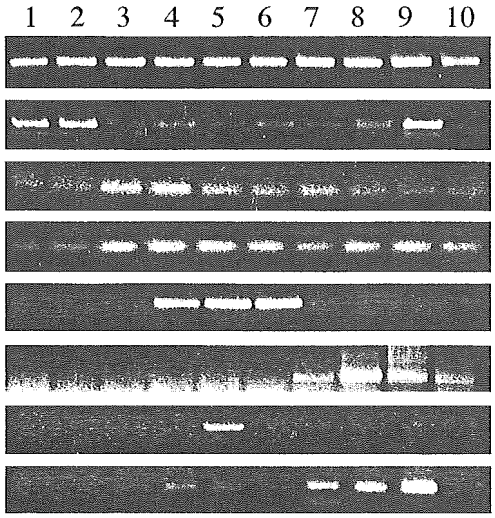

Fig. 5. Expression of various mRNAs related to osteoblast marker in GCTSC and control cells. The expression of β-actin (positive control mRNA), BMP-2, BMP-4, collagen-1, alkaline phosphatase (ALP), osteocalcin and core binding factor 1 (Cbfa1) in HeLa (lane 1), CV-1 cells (lane 2), GCTSC no. 1 (lane 3), no. 2 (lane 4), no. 3 (lane 5), and no. 4 (lane 6), HOS (lane 7), HSOS-1 (lane 8), HS-1 (lane 9) and G292 (lane 10) was analyzed by RT-PCR.

induce osteoclast-like cells from blood monocytes is that the soluble RANKL/ODF/OPGL cleaved by TACE is released from GCTSC and the soluble factor interacts with RANK expressed in monocytes, resulting in osteoclast-like cell formation in co-operation with M-CSF secreted from GCTSC. Furthermore, TIMP-3 controls TACE activity, resulting in regulation of soluble RANKL production.

It is now known that variations in extracellular calcium concentration exert diverse physiologic effects in a variety of tissues that are mediated by a calcium-sensing receptor (CaSR) [9]. Activation of the CaSR represents an important signal transduction pathway in parathyroid tissue, kidney, intestine, placenta, brain, and perhaps bone. In bone, Ca^{2+}, a major extracellular factor in the bone microenvironment during bone remodeling, could potentially serve as an extracellular first messenger, acting the CaSR that stimulates the proliferation of preosteoblasts and their differentiation to osteoblasts. The signaling pathways of high Ca^{2+} were found to be responsible for controlling the expression of RANKL in mouse osteoblastic cells [4]. In this study, the effect of Ca^{2+} on the RANKL expression in GCTSC was investigated. GCTSC expressed the same CaSR as osteoblasts and osteosarcoma-derived cells. Intriguingly, extracellular concentration of Ca^{2+} and the neomycin, agonist of CaSR, stimulated the RANKL expression in GCTSC, while expression levels of OPG and M-CSF were not influenced by these stimulations. These findings suggest that extracellular concentration of

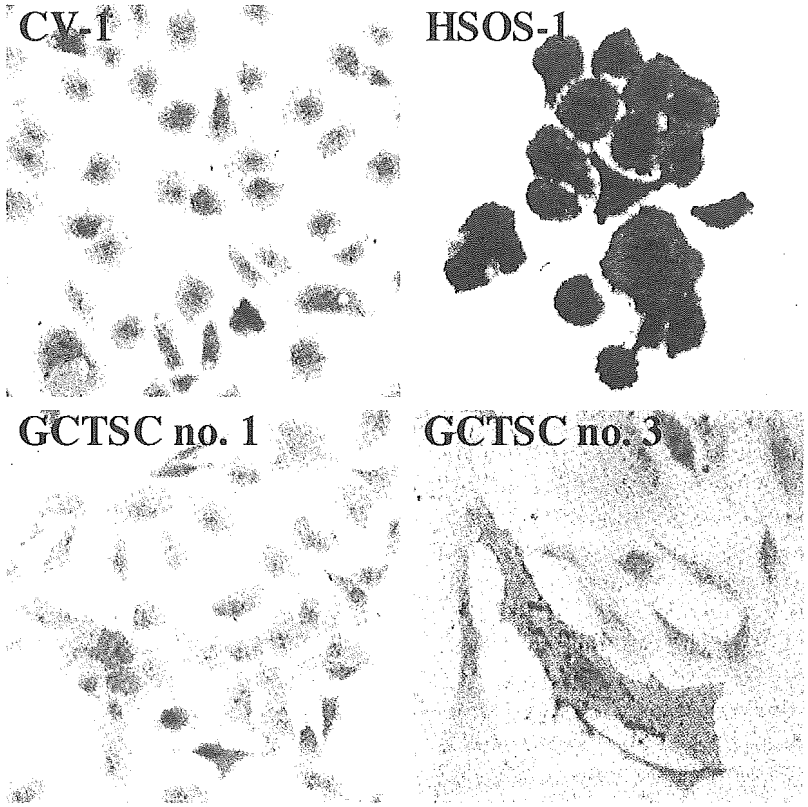

Fig. 6. Alkaline phosphatase staining. Alkaline phosphatase staining was carried out by using CV-1, HSOS-1, GCTSC (no. 1) and GCTSC (no. 3).

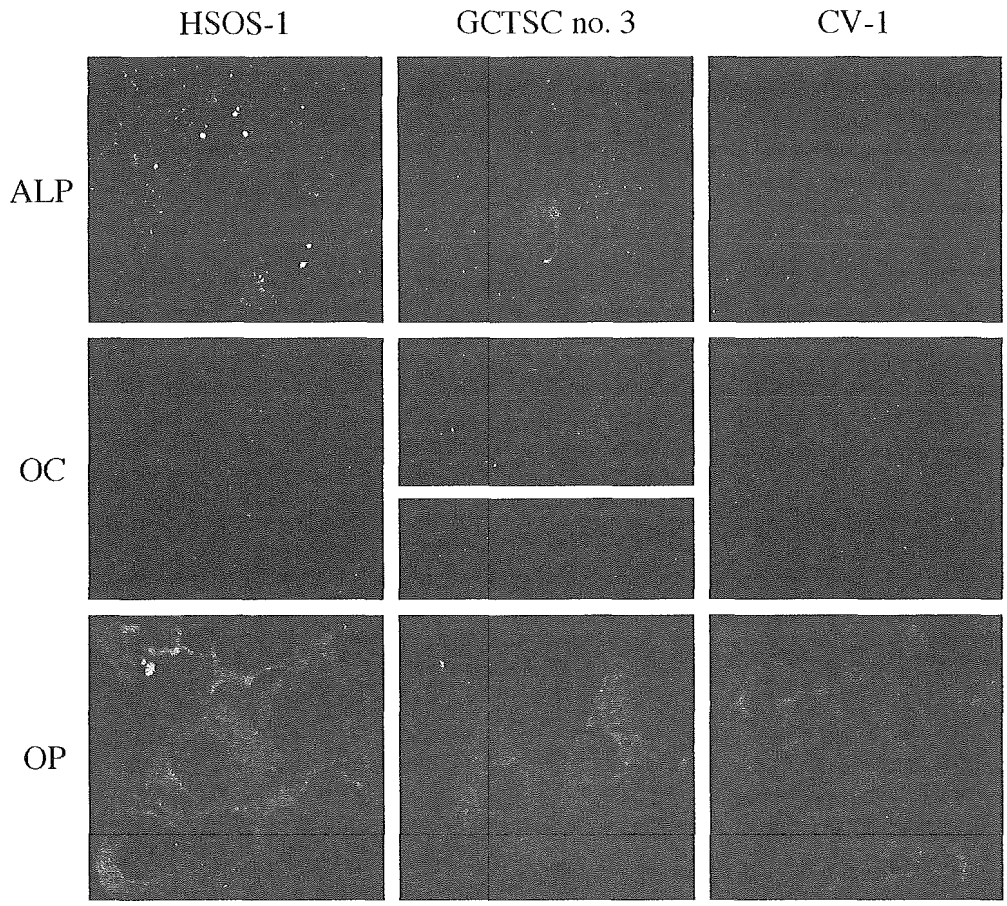

Fig. 7. Immunostaining of osteopontin, bone-specific alkaline phosphatase and osteocalcin. HSOS-1, GCTSC no. 3 and CV-1 cells were immunostained with anti-bone-specific alkaline phosphatase (ALP), anti-osteocalcin (OC) or anti-osteopontin (OP) antibody, and then with FITC-labeled secondary anti-serum.

Ca^{2+} regulates osteoclastogenesis induced by GCTSC via control of the RANKL expression in GCTSC. Chattopadhyay et al. [4] have recently reported that the mitogenic effect of Ca^{2+} on rat calvarial osteoblasts is CaSR-mediated. Kim et al. [16] have also reported that high Ca^{2+} increases the expression of RANKL in mouse osteoblastic cells. However, whether the enhanced expression of RANKL is mediated by CaSR remains unclarified.

In this study, the cytological properties of GCTSC were analyzed. The transcription factor Cbfa1 is a critical regulator of osteoblast differentiation. Cbfa1 mRNA was detected in all of four GCTSC. Osteocalcin gene is truly osteoblast specific and the promoter can be used to unravel the transcriptional control of osteoblast-specific gene. Osteocalcin mRNA could be detected in one GCTSC (no. 3), a part of which was immunostained by anti-osteocalsin antibody. A few cells of GCTSC no. 3 and no. 4 were alkaline phosphatase staining positive and was immunostained by anti-bone specific alkaline phosphatase antibody. BMP-4 and collagen-I mRNAs were expressed at higher levels in GCTSC than those in control cells (HeLa and CV-1 cells). These findings suggest that GCTSC are intimately related to osteoblasts, though potential contamination of GCTSC cell line with oseoblast lineage cells obtained at the time of initial harvesting could not be completely excluded.

In summary, this study suggests that GCTSC having common properties to osteoblasts secrete soluble RANKL which induces osteoclast formation from blood monocytes.

Acknowledgment

This study was supported in part by a Grant-in-Aid for Scientific Research from the Ministry of Education, Culture, Sports, Science, and Technology of Japan and by Mie Medical Research Fund.

References

[1] Amour A, Slocombe PM, Webster A, Butler M, Knight CG, Smith BJ, et al. TNF-α converting enzyme (TACE) is inhibited by TIMP-3. FEBS Lett 1998;435:39–44.

[2] Brecher ME, Franklin WA, Simon MA. Immunohistochemical study of mononuclear phagocytes antigens in giant cell tumor of bone. Am J Pathol 1986;125:252–8.
[3] Byers VS, Levin AS, Johnston JO, Hackett AJ. Quantitative immunofluorescence studies of the tumor antigen-bearing cell in giant cell tumor of bone and osteogenic sarcoma. Cancer Res 1975;35:2520–31.
[4] Chattopadhyay N, Yano S, Tfelt-Hansen J, Rooney P, Kanuparthi D, Bandyopadhyay S, et al. Mitogenic action of calcium-sensing receptor on rat calvarial osteoblasts. Endocrinology 2004;145:3451–62.
[5] Chirgwin JM, Przybyla AE, MacDonald RJ, Rutter WJ. Isolation of biologically active ribonucleic acid from sources enriched in ribonucleases. Biochemistry 1979;18:5294–9.
[6] Clohisy DR, Vorlicky L, Oegema TR, Snover D, Thompson RC. Histochemical and immunohistochemical characterization of cells constituting the giant cell tumor of bone. Clin Orthop 1993; 287:259–65.
[7] Goldring SR, Roelke MS, Petrison KK, Bham AK. Human giant cell tumors of bone-identification and characterization of cell types. J Clin Invest 1987;79:483–91.
[8] Goldring S, Schiller AL, Mankin HJ, Dayer JM, Krane SM. Characterization of cells from human giant cell tumors of bone. Clin Orthop 1986;204:59–75.
[9] Goodman WG. Calcium-sensing receptors. Semin Nephrol 2004;24:17–24.
[10] Hanaoka H, Friedman B, Mack RP. Ultrastructure and histogenesis of giant cell tumor of bone. Cancer 1970;25:1408–23.
[11] Horton MA, Lewis D, McNulty K, Pringle JA, Chamber STJ. Monoclonal antibodies to osteoclastomas (giant cell bone tumors): Definition osteoclast-specific cellular antigens. Cancer Res 1985;45:5663–9.
[12] Horton MA, Pringle JA, Chamber STJ. Identification of human osteoclasts with monoclonal antibodies. New Engl J Med 1985; 312:923–4.
[13] James IE, Walsh S, Dodds RA, Goen M. Production and characterization of osteoclast-selective monoclonal antibodies that distinguish between multinucleated cells derived different human tissues. J Histochem Cytochem 1991;39:905–14.
[14] Jimi E, Akiyama S, Tsurukai T, Okahashi N, Kobayashi K, Udagawa N, et al. Osteoclast differentiation factor acts as a multifunctional regulator in murine osteoclast differentiation and function. J Immunol 1999;163:434–42.
[15] Joyner CJ, Quinn JM, Triffitt JT, Owen ME, Athanasou NA. Phenotypic characterization of mononuclear and multinuclear cells of giant cell tumor of bone. Bone Miner 1992;16:37–48.
[16] Kim YH, Kim JM, Kim SN, Kim GS, Baek JH. p44/42 MAPK activation is necessary for receptor activator of nuclear factor-kappa B ligand induction by high extracellular calcium. Biochem Biophys Res Commun 2003;16:729–35.
[17] Lacey DL, Timms E, Tan HL, Kelley MJ, Dunstan CR, Burgess T, et al. Osteoprotegerin ligand is a cytokine that regulates osteoclast differentiation and activation. Cell 1998;93:165–76.
[18] Lum L, Wong BR, Josien R, Becherer JD, Erdjument-Bromage H, Schlondorff J, et al. Evidence for a role of a tumor necrosis factor-a (TNF-α)-converting enzyme-like protease in shedding of TRANCE, a TNF family member involved in osteoclastogenesis and dendric cell survival. J Biol Chem 1999;274:13613–8.
[19] McLarnon S, Holden D, Ward D, Jones M, Elliott A, Riccardi D. Aminoglycoside antibiotics induce pH-sensitive activation of the calcium-sensing receptor. Biochem Biophys Res Commun 2002; 297:71–7.
[20] Mii Y, Miyauchi Y, Morishita T, Miura S, Honoki K, Aoki M, et al. Ultrastructural cytochemical demonstration of proteoglycans and calcium in the extracellular matrix of chondroblastomas. Ultrastruct Pathol 1991;15:623–9.
[21] Miyamoto N, Higuchi Y, Mori K, Ito M, Tsurudome M, Nishio M, et al. Human osteosarcoma-derived cell lines produce soluble factor(s) that induces differentiation of blood monocytes to osteoclast-like cells. Int Immunopharmacol 2002;2:25–38.
[22] Miyamoto N, Higuchi Y, Tajima M, Ito M, Tsurudome M, Nishio M, et al. Spindle-shaped cells derived from giant cell tumor of bone support differentiation of blood monocytes to osteoclast-like cells. J Orthop Res 2000;18:647–54.
[23] Nicholson GC, Horton MA, Sexton PM, D'Santos CS, Moseley JM, Kemp BE, et al. Calcitonin receptors of human osteoclastoma. Horm Metabol Res 1987;19:585–9.
[24] Pan B, Farrugia AN, To LB, Findlay DM, Green J, Lynch K, et al. The nitrogen-containing bisphosphonate, zoledronic acid, influences RANKL expression in human osteoblast-like cells by activating TNF-alpha converting enzyme (TACE). J Bone Miner Res 2004;19:147–54.
[25] Quinn JM, Elliott J, Gillespie MT, Martin TJ. A combination of osteoclast differentiation factor and macrophage-colony stimulating factor is sufficient for both human and mouse osteoclast formation. Endocrinology 1998;139:4424–7.
[26] Simonet WS, Lacey DL, Dunstan CR, Kelley M, Chang MS, Luthy R, et al. J. Osteoprotegerin a novel secreted protein involved in the regulation of bone density. Cell 1997;89:309–19.
[27] Steiner GC, Ghosh L, Dorfman HD. Ultrastructure of giant cell tumors of bone. Hum Pathol 1972;3:569–86.
[28] Suda T, Takahashi N, Martin TJ. Modulation of osteoclast differentiation. Endocr Rev 1992;13:66–80.
[29] Tabata N, Ito M, Shimokata K, Suga S, Ohgimoto S, Tsurudome M, et al. Expression of fusion regulatory proteins (FRPs) on human peripheral blood monocytes: Induction of homotypic aggregation and formation of multinucleated giant cells by anti-FRP-1 monoclonal antibodies. J Immunol 1994;153: 3256–66.
[30] Tsuda E, Goto M, Mochizuki S, Yano K, Kobayashi F, Morinaga T, et al. Isolation of a novel cytokine from human fibroblasts that specifically inhibits osteoclastogenesis. Biochem Biophys Res Commun 1997;234:137–42.
[31] Udagawa N, Takahashi N, Akatsu T, Sasaki T, Yamaguchi A, Kodama A, et al. The bone marrow-derived stromal cell lines MC3T3-G2/PA6 and ST2 support osteoclast-like cell differentiation in cocultures with mouse spleen cells. Endocrinology 1989; 125:1805–13.
[32] Wulling M, Engels C, Jesse N, Werner M, Delling G, Kaiser E. The nature of giant cell tumor of bone. J Cancer Res Clin Oncol 2001;127:467–74.
[33] Yasuda H, Shima N, Nakagawa N, Yamaguchi K, Kinosaki M, Mochizuki S, et al. Osteoclast differentiation factor is a ligand for osteoprotegerin/osteoclastogenesis-inhibitory factor and is identical to TRANCE/RANKL. Proc Natl Acad Sci USA 1998;95:3597–602.

THE JOURNAL OF BONE & JOINT SURGERY (Br)

■ CASE REPORT

Intraneural metastasis of a synovial sarcoma to a peripheral nerve

A. Matsumine,
K. Kusuzaki,
H. Hirata,
K. Fukutome,
M. Maeda,
A. Uchida

From the Mie University School of Medicine, Mie, Japan

We describe a case of intraneural metastasis of a synovial sarcoma, the first published case of a metastasis of a soft-tissue sarcoma to a peripheral nerve.

Synovial sarcoma is a high grade malignancy, usually occurring in adolescents and young adults between 15 and 40 years of age. It occurs primarily in the para-articular regions of the extremities, usually in close association to tendon sheaths, bursae, and joint capsules.[1] Metastatic lesions develop in half the cases, most commonly in the lung, followed by the lymph nodes and bone marrow.[1] However, there have been no previous reports of intraneural metastasis of synovial sarcoma to a peripheral nerve.

Case report

In January 2001, a 28-year-old man presented with a mass 10 mm in diameter in the right scapular region. Biopsy revealed a spindle-cell neoplasm growing in a fascicular fashion with the vascular pattern of a haemangiopericytoma suggestive of a monophasic synovial sarcoma. Molecular genetic studies performed on frozen-tissue samples using reverse transcriptase polymerase chain reaction (RT-PCR) showed the fusion transcript for SYT-SSX1, confirming the diagnosis of synovial sarcoma. A CT scan of the chest revealed multiple pulmonary metastases. The diagnosis was monophasic synovial sarcoma, with an American Joint Committee for Cancer Staging System classification[2] of T2b, N0, M1, stage IV. After two cycles of pre-operative chemotherapy, a wide excision of the primary tumour was undertaken. The patient received three cycles of post-operative chemotherapy and underwent excision of left pulmonary metastases five months later. He received a further two cycles of chemotherapy and at follow-up 16 months later complained of the acute onset of severe pain in the dorsolateral aspect of the forearm. He developed a complete high radial nerve palsy within five days of the onset of the pain. There was marked tenderness 7 cm proximal to the lateral humeral epicondyle. No abnormality of the radial nerve in the upper arm was identified on MRI and there were no abnormalities on MRI of the brain and cervical spine.

He underwent exploration of the left radial nerve. A 1.5 cm segment of the nerve at the exit of the spiral groove in the lateral third of the humerus was swollen and grey. Histopathology of frozen sections indicated synovial sarcoma and a wide excision of the nerve was performed. Nerve grafting was not undertaken because of the poor prognosis. Also, the patient had refused nerve grafting as functional recovery would take a long time. At pre-operative counselling, he gave informed consent for

A. Matsumine, MD, PhD, Assistant Professor
K. Kusuzaki, MD, PhD, Assistant Professor
H. Hirata, MD, PhD, Associate Professor
A. Uchida, MD, PhD, Professor
Department of Orthopaedic Surgery
K. Fukutome, MD, PhD, Assistant Professor
Department of Pathology
M. Maeda, MD, PhD, Assistant Professor
Department of Radiology
Mie University School of Medicine, 2-174 Edobashi, Tsu-city, Mie 514-8507, Japan.

Correspondence should be sent to Dr A. Matsumine; e-mail: matsumin@clin.medic.mie-u.ac.jp

doi:10.1302/0301-620X.8711.16522 $2.00

J Bone Joint Surg [Br] 2005;87-B:1553-5.
Received 18 March 2005; Accepted 24 May 2005

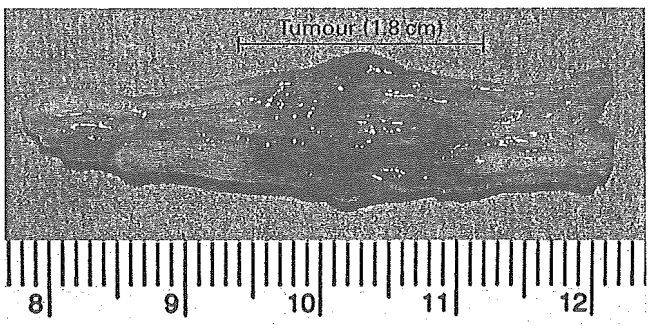

Fig. 1

Lengthwise section of the removed radial nerve.

Fig. 2a

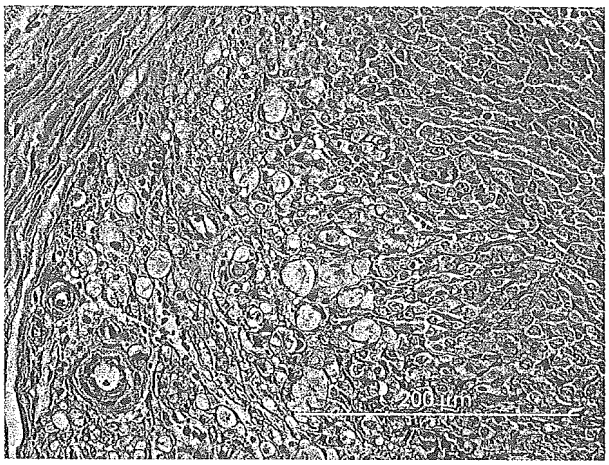

Fig. 2b

Microscopic finding of a transverse section of the radial nerve. Figure 2a – Low magnification view showing infiltration of synovial cells into endoneurieum. Note the intact perineurium (haematoxylin and eosin, x40). Figure 2b – High magnification view showing monophasic synovial sarcoma, identical to the original biopsy (haematoxylin and eosin, x40).

Table I. Case reports of intraneural metastasis of malignancy to the peripheral nerve of extremities

Authors	Gender*/ age	Location	Diagnosis	Symptom	Utility of the images for diagnosis†	Treatment‡	Recovery of palsy†	Pain relief†	Oncological status§
Lusk, Kline and Garcia[6]	F/26	Brachial plexus	Melanoma	Pain	ND	S	ND	N	NED
van Bolden et al[8]	M/60	Radial nerve	Lymphoma	Palsy	ND	S, RT	N	-	NED
Artico et al[3]	F/66	Brachial plexus	Breast cancer	Pain, palsy	N	S, C	N	Y	NED
Kline and Hudson[5]	ND	Brachial plexus	Melanoma	ND	ND	S, RT	ND	ND	ND
	ND	Brachial plexus	Melanoma	ND	ND	S, RT	ND	ND	ND
Meller et al[7]	M/65	Brachial plexus	Laryngeal cancer	Pain, palsy	N	S, C	N	Y	NED
	F/42	Brachial plexus	Breast cancer	Pain, palsy	N	S, RT	N	Y	NED
	F/52	Brachial plexus	Breast cancer	Pain, palsy	N	S, C	N	Y	NED
	F/32	Brachial plexus	Breast cancer	Pain, palsy	N	S, C	N	Y	NED
	M/45	Brachial plexus	Lymphoma	Pain, palsy	N	C, RT	N	Y	DOD
Cantone, Rath and Richter[4]	M/50	Sciatic nerve	Melanoma	Pain, palsy	MRI	S, RT	N	Y	NED

* F, female; M, male
† ND, not determined; N, No; Y, yes
‡ C, chemotherapy; RT, radiotherapy; S, surgery
§ DOD, dead of disease; NED, no evidence of disease

a functional orthosis for the predicted permanent radial nerve palsy. Macroscopic examination of the excised radial nerve showed that tumour tissue occupied about 4/5 of the cross-section of the nerve, and occupied a 1.8-cm length of the longitudinal section (Fig. 1) and histopathology confirmed an identical appearance to the synovial sarcoma which had originally been removed from the right scapular region (Fig. 2).

Although the intractable neuralgia resolved the patient subsequently died from metastatic pulmonary disease about 18 months later.

Discussion

A common neurological complication in advanced stages of various malignancies is direct invasion of cranial nerves, the epidural space, or spinal nerve roots. However, intraneural metastasis to peripheral nerves is very rare. Eleven cases have been reported (Table I).[3-8] There have been no reports of intraneural metastasis of synovial sarcoma to a peripheral nerve.

The metastatic process consists of various stages of detachment, migration, arrest in the target organ, formation of micrometastases, and vascular neogenesis leading to overt tumour formation.[9] Why is a metastasis of a tumour to a peripheral nerve so rare? The axonal environment in the endoneurium of the peripheral nervous system is isolated from the general extracellular space of the body by a diffusion barrier called the blood-nerve barrier, which is similar to the blood-brain barrier.[10] The blood-nerve barrier consists of tight and adherence junctions, both between perineural and endothelial cells in the endoneurium.[10] It appears that the blood-nerve barrier is responsible for the resistance to metastatic implantation[7] of this peripheral, but highly vascularised, tissue. In the present case, it is sug-